M.SC.

UNG

This is to certify that the

thesis entitled

DYNAMIC RECRYSTALLIZATION OF BORON DOPED Ni_3Al POLYCRYSTAL DURING HIGH TEMPERATURE COMPRESSION TEST

presented by

Hang-Fei Yung

has been accepted towards fulfillment
of the requirements for

M.S. degree in Metallurgy

Major professor
Professor G. Gottstein

Date 2-24-89
February-24-1989

DYNAMIC RECRYSTALLIZATION OF BORON DOPED Ni_3Al POLYCRYSTAL DURING HIGH TEMPERATURE COMPRESSION TEST

BY

HANG - FEI YUNG

A THESIS

Submitted to

Michigan State University

in partial fulfillment of the requirements

for the degree of

MASTER OF SCIENCE

Department of Metallurgy, Mechanics and

Materials Science

1989

ABSTRACT

DYNAMIC RECRYSTALLIZATION OF BORON DOPED Ni_3Al POLYCRYSTAL DURING HIGH TEMPERATURE COMPRESSION TEST

BY

HANG-FEI YUNG

The features of dynamic recrystallization (DRX) of Ni_3Al and pure Ni during compression at temperature between 0.5 - 0.8 of the melting temperature (Tm) and strain rate between 2×10^{-3} S^{-1} and 2×10^{-5} S^{-1} were studied. From the metallographic observation and stress - strain behavior, it was found that DRX actually occured during high temperature deformation. For the given deformation condition only a single maximum of the flow curve was observed for Ni_3Al, while an oscillation flow behavior was found for Ni. The microstructure of Ni_3Al always underwent grain refinement, while the microstructure of Ni underwent grain coarsening during DRX. The observations are in line with the prediction that a transition from sigle peak to multiple peak flow behavior only occurs for D_o / $2D_S$ = 1. For Ni an activation analysis of σ_R yielded a strss exponent, n = 6.8. and an activation energy, Q = 57.79 kcal / mole. An activation analysis for Ni_3Al was not feasible since n and Q depend on temperature.

ACKNOWLEDGEMENTS

I am grateful to my advisor, Professor G.Gottstein, for his kindly instruction and necessity support for experiment. Also, I would like to thank my colleague, S.R.Chen, for his technical assistance and discussion and others who exchanged view on the DRX experiment.
Finally, I would like to appreciate my wife for her mental support and fortitude during the past two years.

TABLE OF CONTENTS

LIST OF TABLES

LIST OF FIGURES

Figure Captions — Page

1. INTRODUCTION

The dynamic recrystallization (DRX) of the material with $L1_2$ structure such as Ni_3Al [1] and Zr_3Al [2] has been reported to explore the fracture mode by using tension test.

In order to observe the kinetic of the grain growth under DRX process of the Ni_3Al, we chose various compression test conditions and prepared two different initial grain sizes (D_o). Controlling Z value and D_o, we supposed that the transition of DRX flow curve for Ni_3Al from continuous to periodic should be taken place because lower Z value and smaller D_o tend to the occurrence of multipeak. Finally, we found that the behavior of the DRX can be related to the recrystallization stress (σ_R) and the final grain size (D_S) has relationship to the steady-state flow stress (σ_S).

The DRX behavior of pure Ni was compared with Ni_3Al because Ni_3Al has a large amount of Ni and the similarity of the melting temperature (Tm), i.e. 1395°C, 1450°C, also to inspect the D_o is independence of D_S .

2 LITERATURE SURVEY

Materials would soften due to the recrystallization while they are subjected to deform at high temperature, above half of the melting temperature, which called dynamic recrystallization (DRX).

Since 1939, the topic of DRX has been mentioned in the creep test of Pb [3]. Up to now, several reports in this field have been stated in various deformation tests, such as torsion test [4,5,6,7,8,9], tension test [1,2,10,11], rolling test [12,13,14], and compression test [15,16,17,18]. According to these authors, the most remarkable phenomenon when material is deformed at elevated temperature with given strain rate ($\dot{\varepsilon}$) is the flow stress-strain (σ-ε) curve with a characteristic shape, either periodic (multipeak) or continuous (single peak) (Fig. 1) [3].

This dynamic-softening process is thermal-activated, giving a dependence of σ on $\dot{\varepsilon}$ and temperature which can be expressed in terms of the Zener-Hollonom parameter, Z, (Fig. 2) [18]

$$Z = \dot{\varepsilon} \exp (Q/RT)$$

where, Q is activation energy. The style of the flow curve can be changed from periodically to continuously as the Z value is increased. On the other words, when the Z is decreased the flow curve shows from single peak to multipeak. Therefore, when the temperature is decreased or the $\dot{\varepsilon}$ is increased, the single peak will occur and the multipeak takes place with increasing temperature or decreasing $\dot{\varepsilon}$.

Correspond to the initial grain size (D_o)and steday-state recrystalized grain size (D_S), when the oscillation flow curve appears, the grain coarsening occurs ($D_o << D_S$), and when the continuous flow

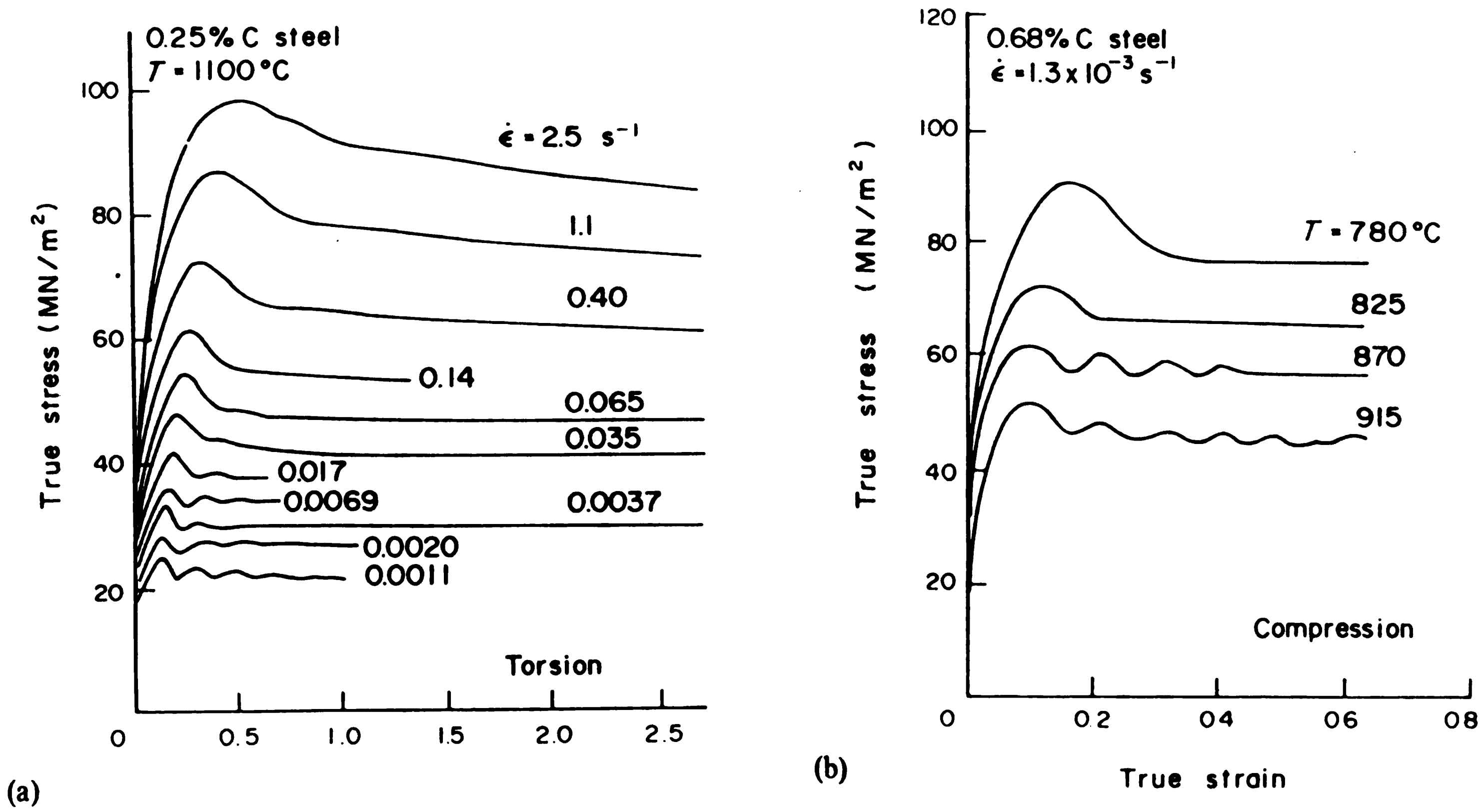

Fig. 1. (a) Effect of strain rate on the flow curves. (b) Effect of temperature on the flow curves [3].

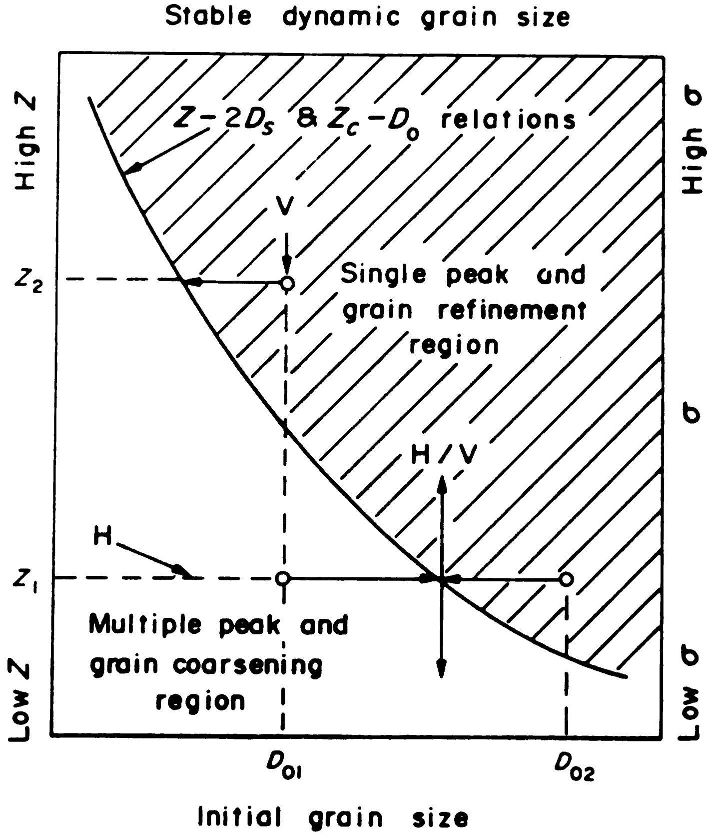

Fig. 2. A microstructure mechanism map for distinguishing between the occurrence of two types of DRX[18].

curve shows means the specimen is undergoing grain refinement ($D_o >> D_S$).

2.1 Effect of Strain Rate on Grain Size of DRX

When the material undergoes DRX, the dislocations substructure develops in the initial stage of deformation which means the new cell structure is smaller and has more tangled cell walls [18].

At higher $\dot{\varepsilon}$, a finer tangled cellular structure is developed throughout all the grain, which does not leave grain boundary segment long enough to bulge. With increasing strain, some tangles build up to high misorientations, the nuclei create within each grain. The density is higher near the grain boundary because the higher strain. By the time, steady-state flow is attained, new small equiaxed grains have replaced the original ones.

According to the Fig. 3a [3], before recrystallization (RX) is complete, the region which first recrystallized reaches the critical strain for a second nucleation. Under this condition, the dislocation densities at the center of the recrystallized grains have increased with further straining the material, which tend to grow another nuclei. Because nucleation or necklace structure occurs at the existing boundaries, the dynamic grain size attains the final stable dynamic grain size(D_S). Therefore, continuous deformation results in work hardening to take place within the dynamic recrystallized grains and reducing the driving force for growth. Hence, the final stable grain size is refined, and leaves a single peak stress - strain curve.

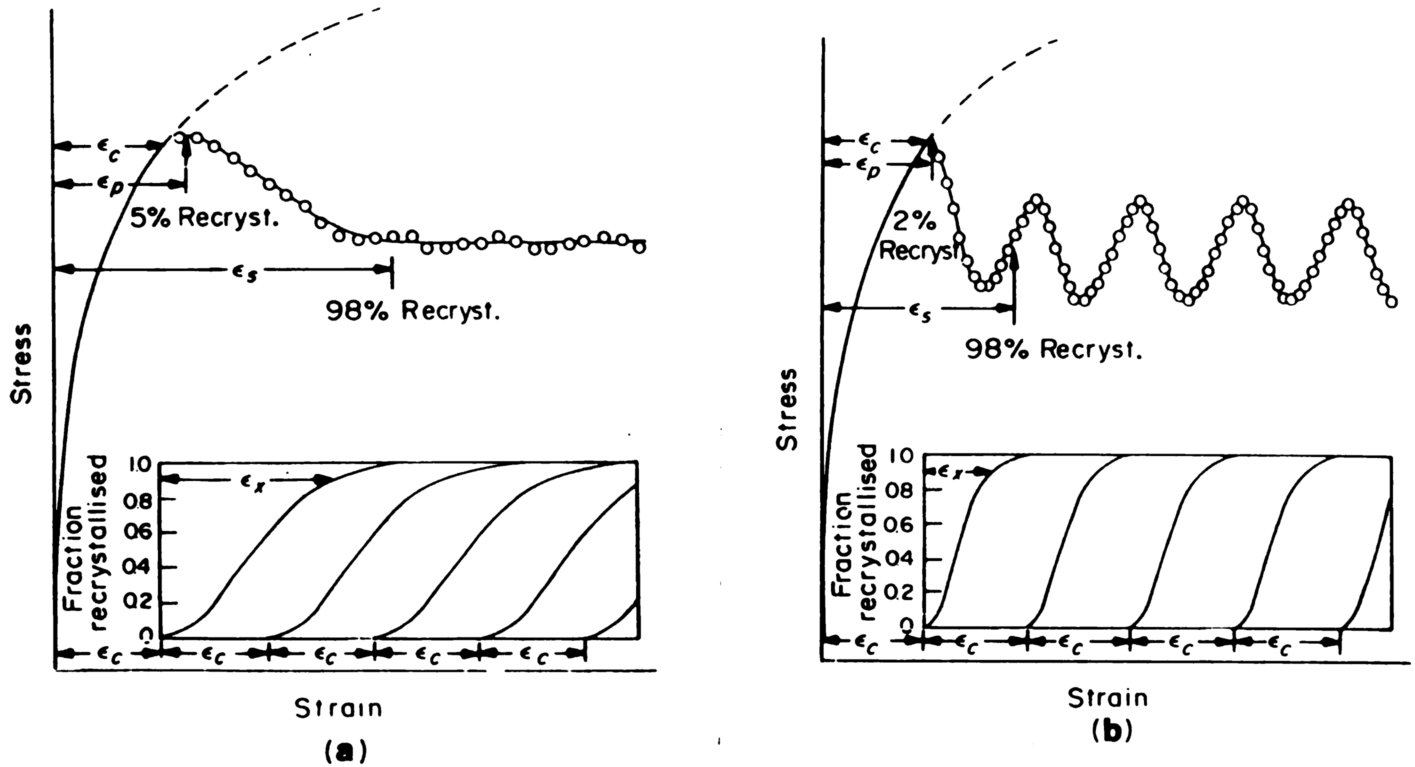

Fig. 3. Predicted stress - strain curves for DRX. (a) A steady state curve for the condition when $\varepsilon_c < \varepsilon_x$. (b) a cyclic flow curve when the $\varepsilon_c > \varepsilon_x$ [3].

Conversely, at lower strain rate, the grain undergoes coarsening due to nucleation production by bulging of the pre-existing grain boundary. In this case, the impingement of boundary results in the termination of a new dynamic grain growth. From the observation of stress-strain curve (Fig. 3b), the nucleation of all new grains occur at when $\varepsilon > \varepsilon_x$ [ε_c: critical strain for the initiation of RX, ε_p : peak strain for RX, ε_x : strain for the completion RX]. Therefore, the growth is restricted to the region ε_x until the material reaches another RX can be initiated. Hence, one RX cycle is virtually complete before the next cycle starts and results in a multipeak stress-strain flow curve.

However, normally higher strain rate gives rise to higher flow stress, or vice versa [4,10]. Thus, when the material is subjected to deform with lower strain rate at high temperature, the RX stress, σ_R, is lower than at high strain rate under the same test condition and shows periodic σ - ε curve [4].

2.2 Effect of Temperature on the DRX Grain Size

First of all the test temperature for RX should be higher than 1/2 Tm at least. As has been mentioned previousely, temperature has something to do with DRX because of the Z value.

At given $\dot{\varepsilon}$, the Z value will be increased as temperature is decreased which results in a single peak stress-strain curve. Because a higher density of nuclei is given rise to the increasing in subgrain density as the Z value increases [18]. Inversely, increasing temperature at given strain rate will increase the RX process [13] and decrease the Z value which results in a multipeak behavior and the appearance of the grain coarsening. Also, σ_R the decreases as the temperature increases which can be described in terms of the empirical relation [11],

$$\sigma_R = A\ \dot{\varepsilon}^{1/m}\ \exp\ (U/mKT)$$

where, A, m, U are constants. Therefore, RX is periodic at lower stress when temperature is increased, and becomes continuous with increasing stress when temperature is decreased [4].

2.3 Microstructure Change Corresponds to the DRX

The effects of strain rate and temperature on the DRX have been discussed a while ago. Both effects have mentioned one important feature, that is microstructure change, either grain coarsening or refinement, under different test conditions. Also, the shape of the DRX stress-strain curve is dominated by the final grain size. In case grain coarsening (D_o << D_S)takes place, the curve shows periodically and grain refinement (D_o >> D_S) pans up a continuous curve. From the map (Fig. 2), however, changing the D_o seems that the shape of the flow curve can be altered. Thus, it is to be expected that the rate of DRX process decreases, i.e the transition from periodic to continuous behavior, with increasing D_o [15]. Nevertheless, it is found that the domination element, D_S ,is normally related to the σ_S , in terms of

$$\sigma_S = \sigma_o + AD^{-n}$$

where, σ_o, A, n are constants. Formularily, σ_S is only dependent of D_S but D_o [8]. Changing D_o will not affect the shape of the flow curve. However, it increases the probability of the transition. It is clear that decreasing the D_o will increase the rate of the RX and decrease the flow stress of RX.

It is not necessary, however, that D_S should be larger than D_o to produce an oscillation curve. Sakai et al. [3,18] cited the criterion for the transition, $D_o / 2D_S = 1$. Under this example, the oscillation flow curve occurred when we found that $D_S < D_o < 2D_S$, it is considered that the grain coarsening take place due to the small final grains resulting from the growth of the RX nuclei.

3. EXPERIMENTAL PROCEDURES

The material, Ni_3Al, with composition Ni-76,Al-24 and B-0.24 a/o, was supplied by Oak Ridge National Lab.

The pure Ni was ordered from Materials Research Corporation with Ag, Al, Cu, Fe, K, Li, Mg, Mo, Pb, Si, Sn, Ti, V, Zr less than 10 ppm, O-14ppm and N-1ppm.

3.1 Machine

The expriment machine is MTS 810 with 458.20 microconsol which was linked to Znith AT personal computer to remote control the MTS unit and to record the data. The vacuum furnace was set up on the MTS with Centorr S60 - 26350 temperature control unit. The thermocouple was placed at the edge of the cental ceramic rod.

3.2 Specimen Preparation

As-casted Ni_3Al was machined to 5 mm height and 3 mm diameter cylinder by using electric discharge machine (EDM). To keep a normal stress on the surface when applied axisymetric compression load, the sample surfaces were grinded to very flat with flatness no larger than 1/1000 and very perpendicular to the cylindric surface, i.e. aligned by the EDM. All of the specimens were annealed at 800°C for 4 hours in the vacuum furnace at a pressure of approximately 10^{-5} Torr, and allow us to get a grain size with 170 μm (Fig. 4). The small grain size sample, with 9 μm (Fig. 5), was obtained from the above material with large

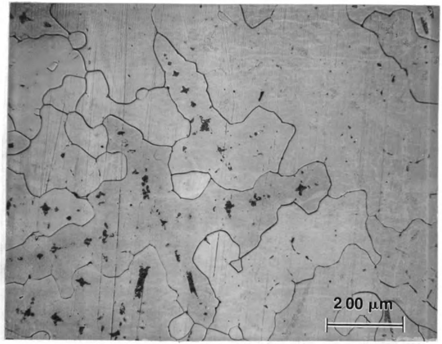

Fig. 4. The metallograph of Ni_3Al annealed at 800°C for 4 hours.

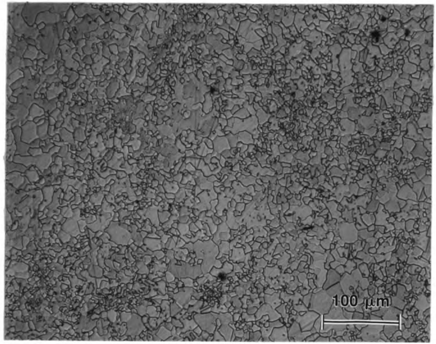

Fig. 5. The metallograph of prestrained Ni_3Al (60 %) annealed at 800°C for 1 hour.

grain size which was undergone the compression test with strain rate = $2 \times 10^{-4} S^{-1}$ at room temperature initially, then, annealed at 800°C for 1 hour in vacuum(about 10^{-6} Torr).

The Ni specimen, with 10.62 mm long, for compression test was cut from pure Ni rod (dia. = 6.35 mm) by diamond saw with speed 150 rpm, and annealed at 1000°C for 30 min in vacuum furnace to get 136 μm (Fig. 6) initial grain size. The result of thermal equilibrium, i.e. at 1000°C, for 1 hour, seems little effect on the initial grain size (Fig. 7).

3.3 Mechanical Test

The Ni_3Al specimens with larger grain size for DRX experiment were compressed at 650°C, 750°C, 850°C,and 1000°C with three strain rate($2 \times 10^{-3} S^{-1}$, $2 \times 10^{-4} S^{-1}$, $2 \times 10^{-5} S^{-1}$). The Ni_3Al samples with smaller grain size were tested at 600°C with stain rate = $2 \times 10^{-4} S^{-1}$, 750°C with strain rate = $2 \times 10^{-4} S^{-1}$, 800°C with strain rate = $2 \times 10^{-3} S^{-1}$,$2 \times 10^{-4} S^{-1}$ and $7 \times 10^{-5} S^{-1}$,as well as 850°C with strain rate = $2 \times 10^{-4} S^{-1}$.

The Ni specimens were compressed at 650°C with strain rate = $2 \times 10^{-4} S^{-1}$, 850°C with strain rate = $2 \times 10^{-3} S^{-1}$,$2 \times 10^{-4} S^{-1}$and $2 \times 10^{-5} S^{-1}$, and 1000°C with stain rate = $2 \times 10^{-4} S^{-1}$.

In order to get thermal equilibrium among the grips, spacers and samples at test temperature, all samples were loaded in the vacuum furnace about 1 hour. The cooling process is after deformation.

3.4 Microstructure Observation

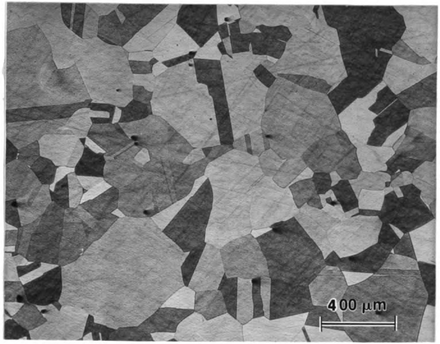

Fig. 6. The metallograph of pure Ni annealed at 1000°C for 30 min.

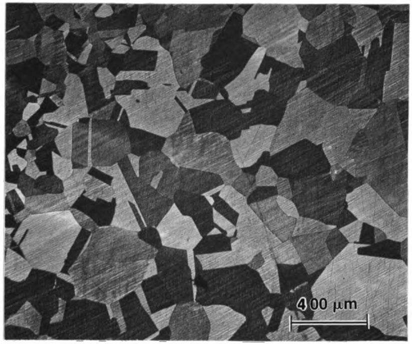

Fig. 7. The metallograph of pure Ni when waited for the thermal equilibrium at 1000°C for 1 hour.

After the accomplishment of the DRX test, the Ni_3Al samples were grinded out about 1mm in order to observe the inner structure and polished by LECO VP-50 autopolisher, i.e. from GRIT 600 to 0.3 micron. The specimens for microscopic examination were, then, immerged in the etching reagent, reagent marbles, which has the following composition,

$CuSO_4$	5g
HCl	20 ml
H_2O	20 ml

at 25°C for 10 seconds.

The Ni for metallographic observation were cut by diamond saw with 150 rpm and polished by LECO autopolisher, then, etched by the following solution,

Nitric Acid	67 ml
Glacial Acetic Acid	33 ml
Hydrochloric Acid	1 ml

at 25°C for 4 seconds

3.5 Protection

In order to protect the grips of the test machine during high temperature, we made two stainless steel spacers and inserted Al_2O_3 thin plat (about 1mm) between the grips and the spacers. Meanwhile, to protect the spacers, we put the Al_2O_3 thick plates (about 3mm) and Al_2O_3 rods (10mm height, 12.5mm dia.) and smeared BN powder on the touching surfaces of the rods and specimens.

4. RESULTS

4.1 The True Stress - True Strain Curve

The experiment results for Ni_3Al with D_o = 170 μm (Fig. 4) at 650°C - 1000°C (T/Tm = 0.55 - 0.76) can be observed that almost all curves (Fig. 8 - 11) undergo the maximum stress which mean the DRX to be initiated, then, drop to certain stresses and keep a steady state flow stress (σ_S). The DRX curves show single peak due to very large D_o . From the Table 1, the effect of strain rate and temperature on the DRX indicates that higher strain rate and lower temperature gives rise to higher σ_R and σ_S .Fig. 8 - 11 show the strain rate effect and Fig. 12 - 14 show the temperature effect.

For the Ni_3Al with fine initial grain size (D_o = 9 μm) the DRX flow curves (Fig. 15,16) show only single peak and, like larger D_o, σ_R and σ_S have the same relationship to strain rate and temperature, i.e. higher strain rate and lower temperature result in a higher flow stress (Table 2). Only the single peak shows up for Ni_3Al is associated with the connection of D_o and D_S . We will discuss below.

For pure Ni with D_o = 136 μm, it reveals the multipeak DRX process (Fig. 17, 18), and same results for σ_R and σ_S (Table 3) under our test conditions.

4.2 Metallographic Examination

When material undergoes the DRX process the D_S affects the type of the flow very much. For the Ni_3Al with D_o = 170 μm, the necklace

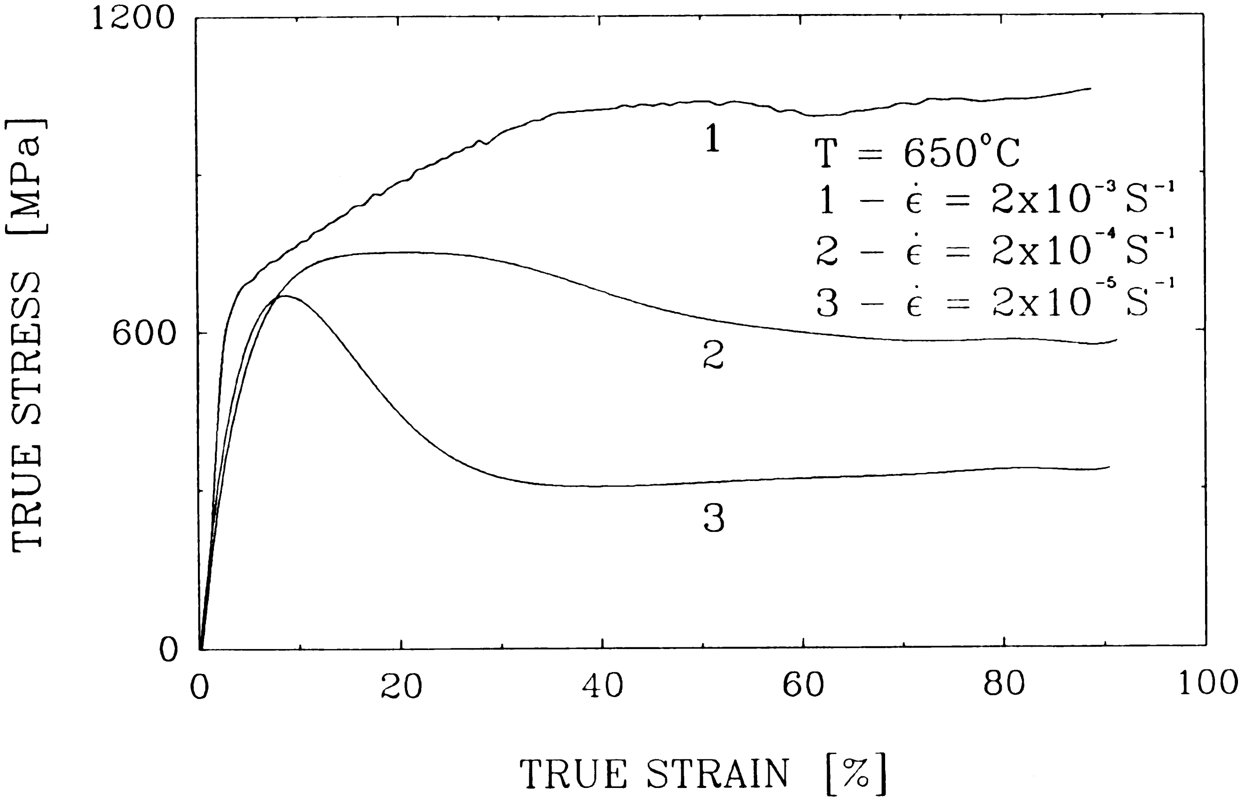

Fig. 8. The flow curves of Ni_3Al (D_o = 170 μm) which were compressed at 650°C with various strain rates.

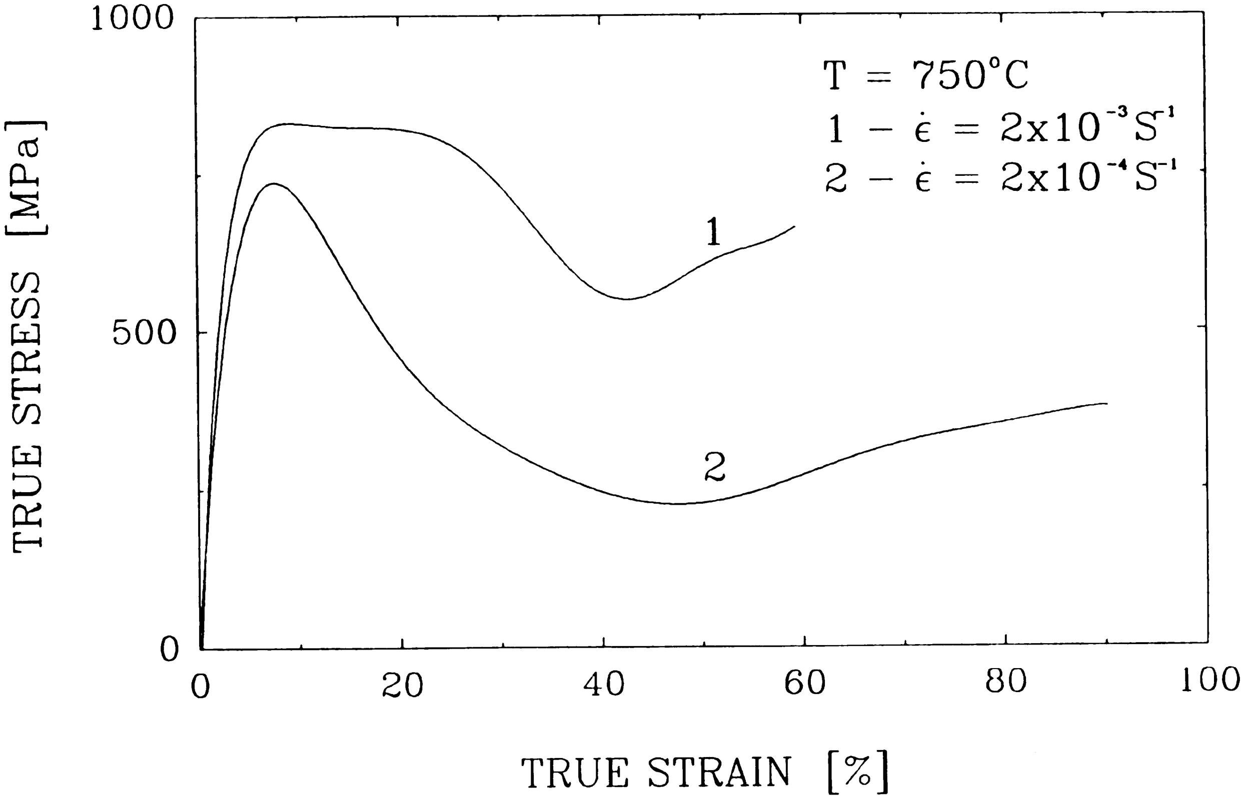

Fig. 9. The flow curves of Ni_3Al (D_o = 170 μm) which were compressed at 750°C with various strain rates.

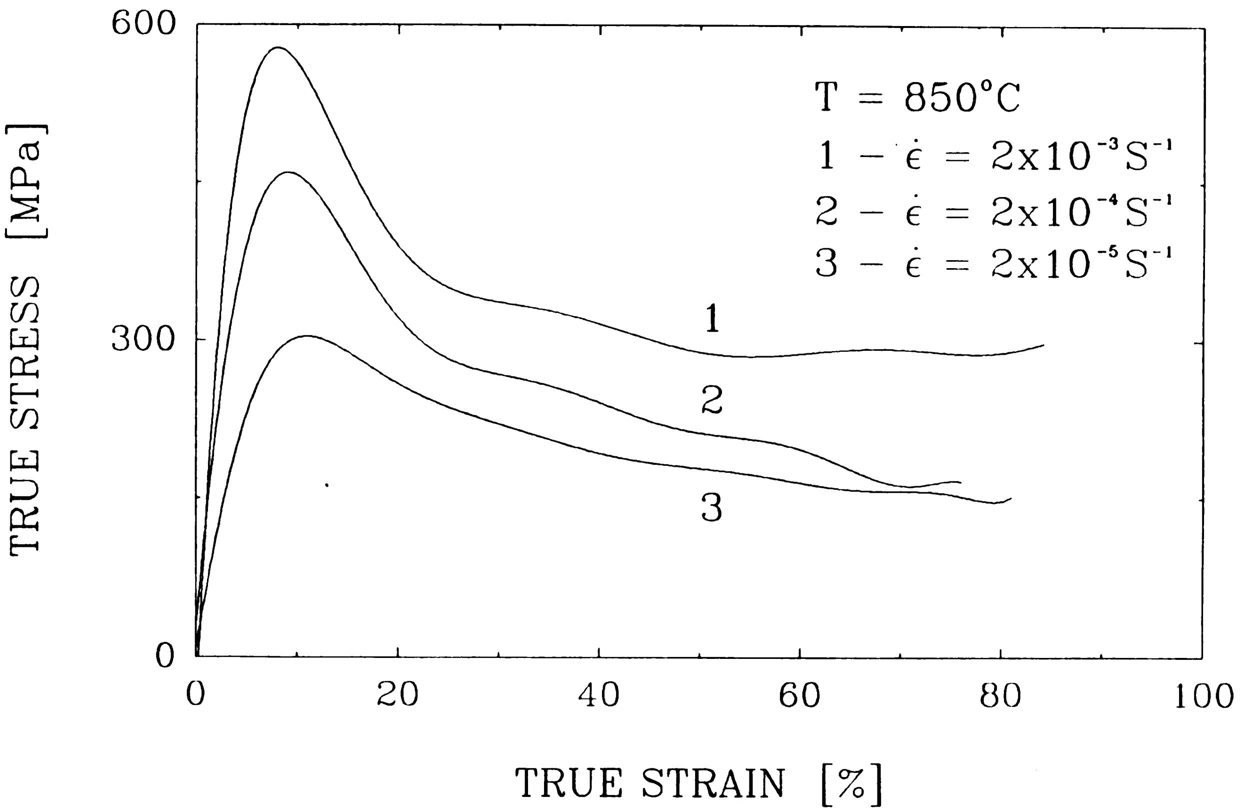

Fig. 10. The flow curves of Ni_3Al (D_o = 170 μm) which were compressed at 850°C with various strain rates.

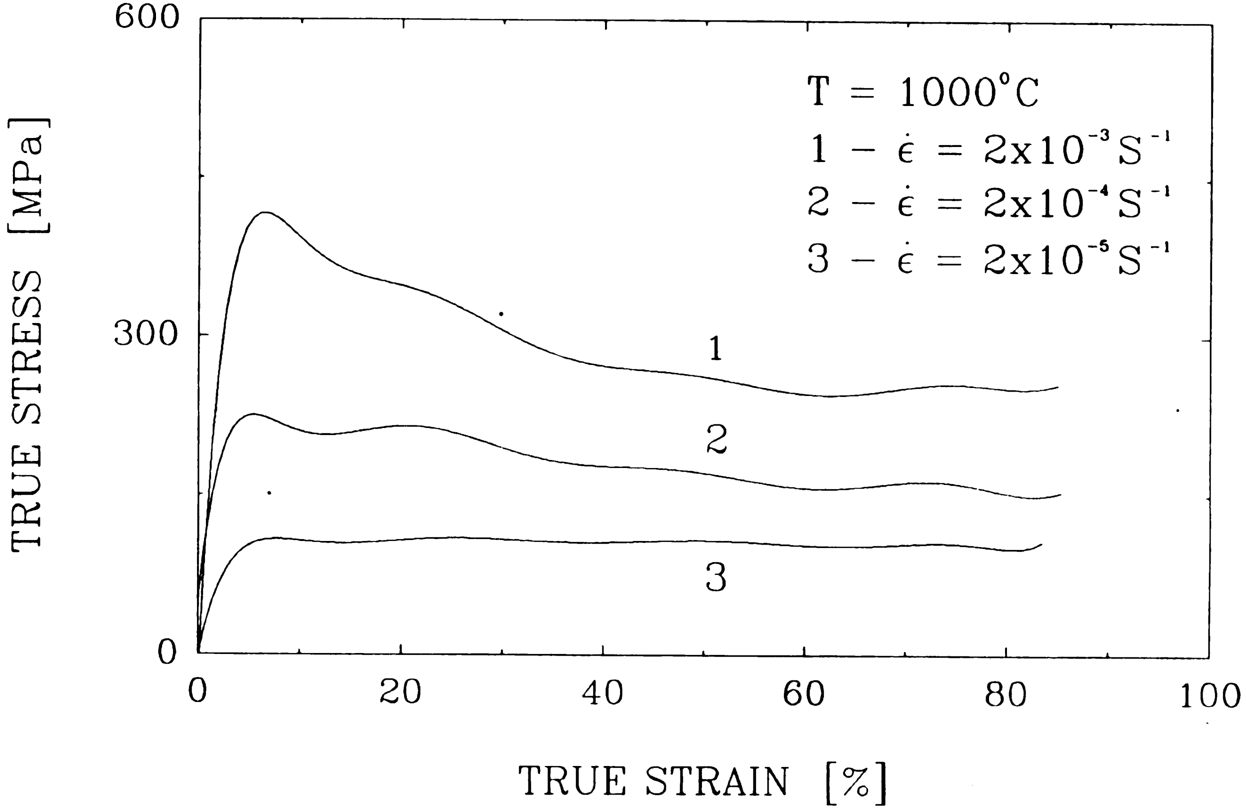

Fig. 11. The flow curves of Ni_3Al (D_o = 170 μm) which were compressed at 1000°C with various strain rates.

Table 1. The σ_R & σ_S under various test condition for Ni_3Al with D_o = 170 μm

σ_R (σ_S) / T°C \ $\dot{\varepsilon}$	$2x10^{-3}s^{-1}$	$2x10^{-4}s^{-1}$	$2x10^{-5}s^{-1}$
650	1035 (1096)	757 (584)	694 (348)
750	833 (660)	703 (422)	---
850	593 (295)	462 (195)	319 (144)
1000	408 (258)	219 (159)	114 (110)

Note: The unit for σ_R & σ_S is MPa.

Table 2. The σ_R & σ_S under various test condition for Ni_3Al with D_o = 9 μm.

σ_R (σ_S) / T°C \ $\dot{\varepsilon}$	$2x10^{-3}s^{-1}$	$2x10^{-4}s^{-1}$	$7x10^{-5}s^{-1}$
600	---	837 (781)	---
750	---	536 (485)	---
800	479 (421)	330 (293)	298 (256)
850	---	228 (194)	---

Note: The unit for σ_R & σ_S is MPa.

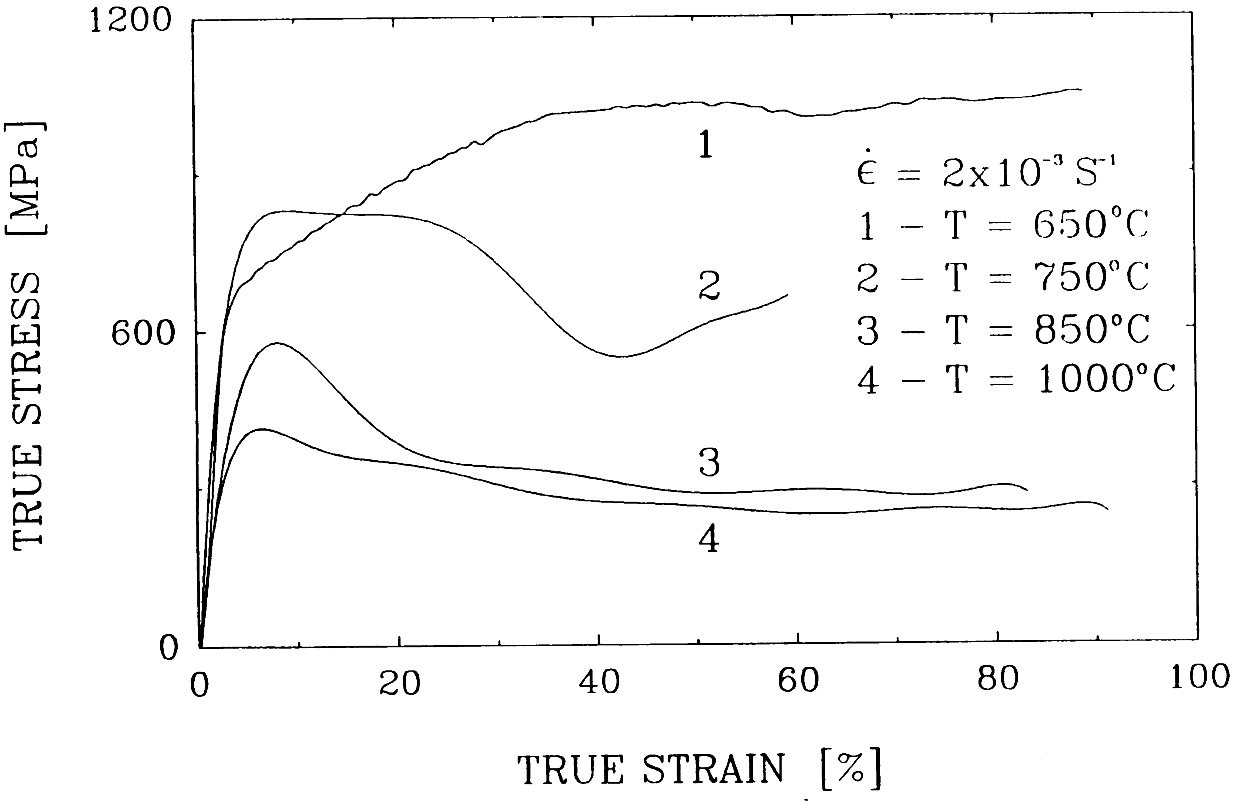

Fig. 12. The flow curves of Ni_3Al (D_o = 170 μm) which were compressed with strain rate 2 x $10^{-3}S^{-1}$ at various temperatures.

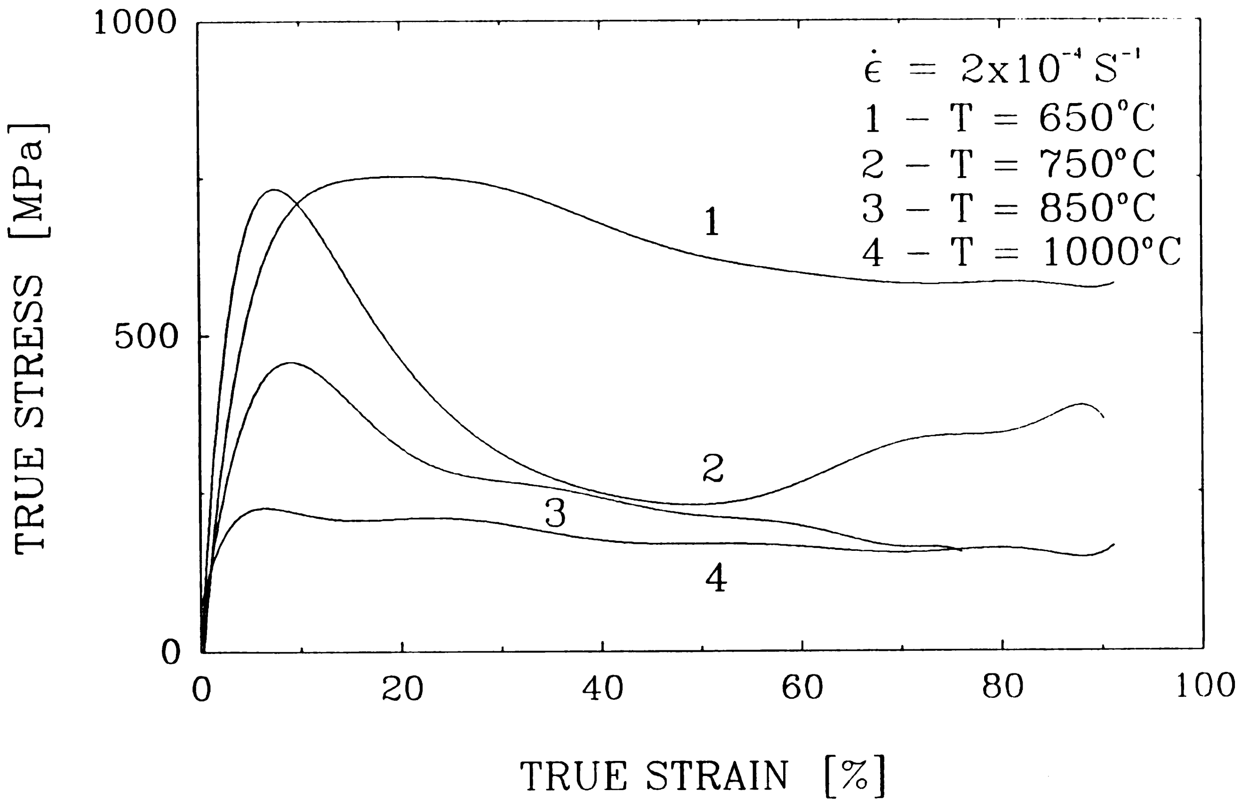

Fig. 13. The flow curves of Ni_3Al (D_o = 170 μm) which were compressed with strain rate 2 x $10^{-4}S^{-1}$ at various temperatures.

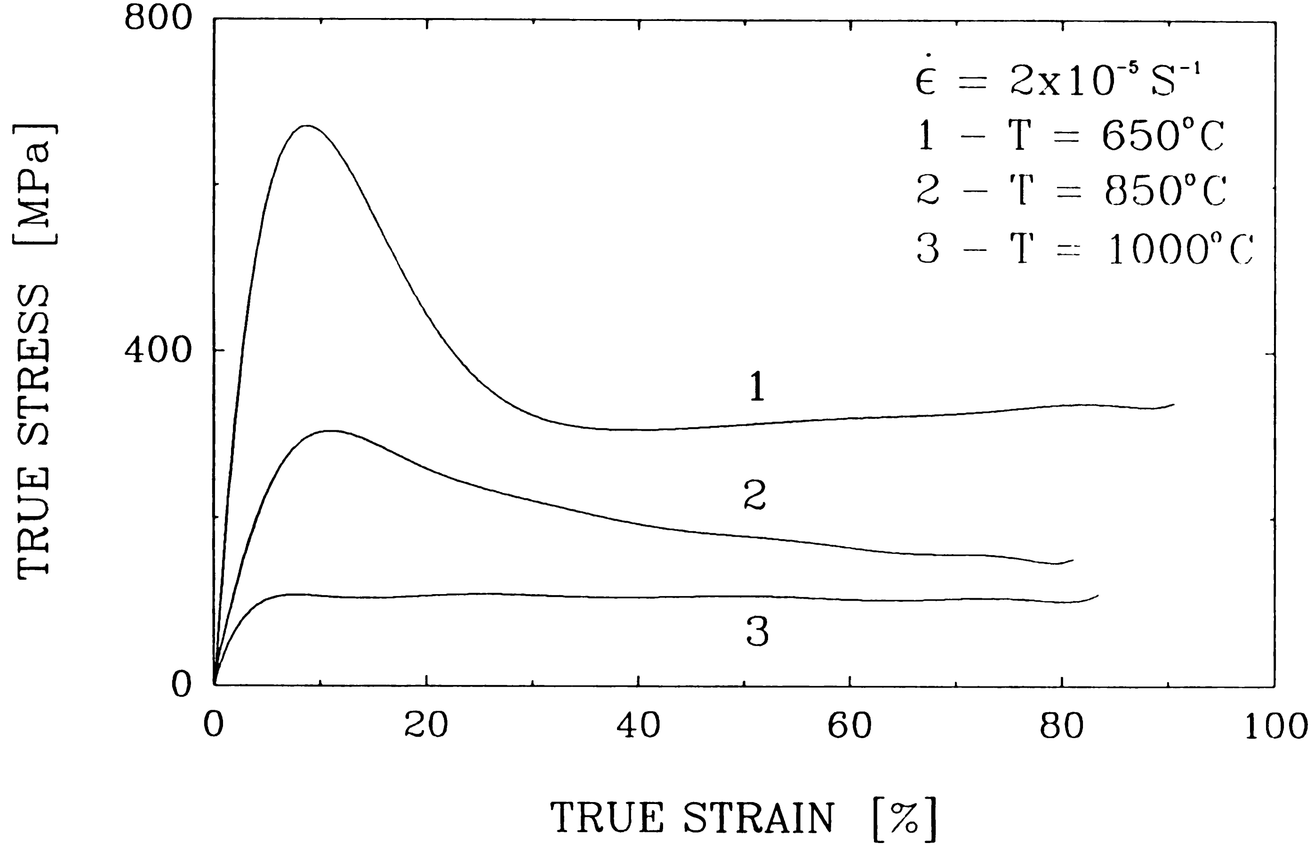

Fig. 14. The flow curves of Ni_3Al (D_o = 170 μm) which were compressed with strain rate 2 x $10^{-5}S^{-1}$ at various temperatures.

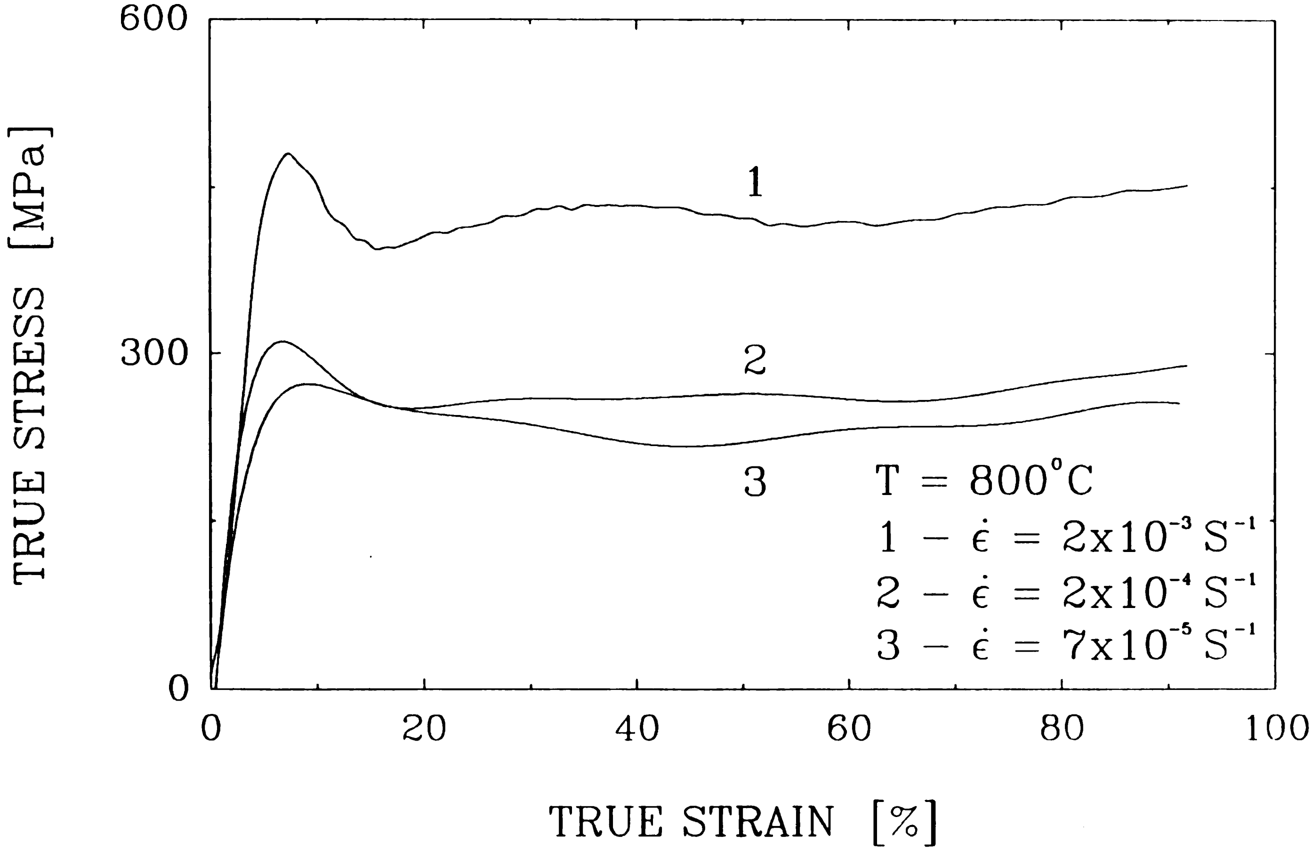

Fig. 15. The flow curves of Ni_3Al (D_o = 9 μm) which were compressed at 800°C with various strain rates.

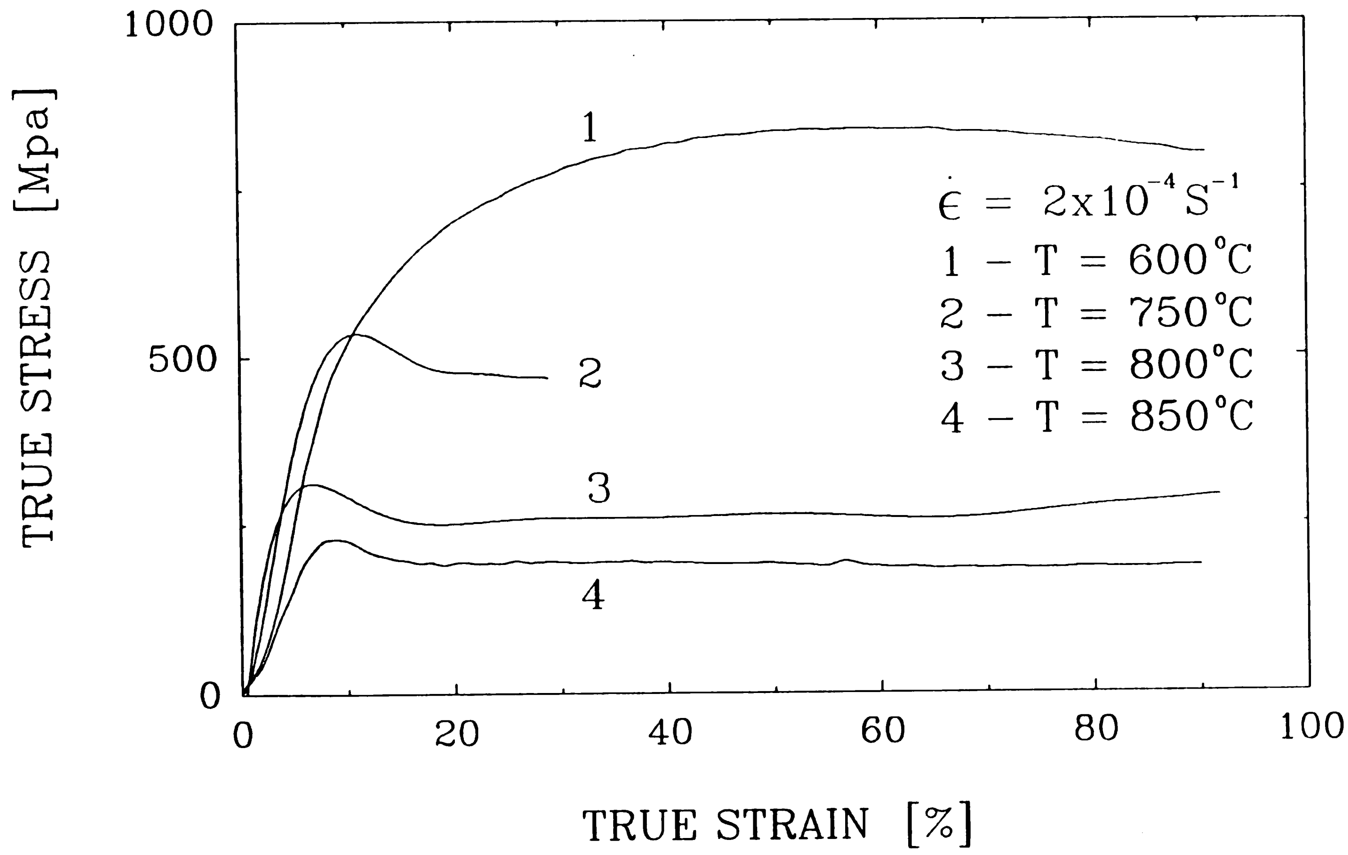

Fig. 16. The flow curves of Ni_3Al (D_o = 9 μm) which were compressed with strain rate $2 \times 10^{-4} S^{-1}$ at various temperatures.

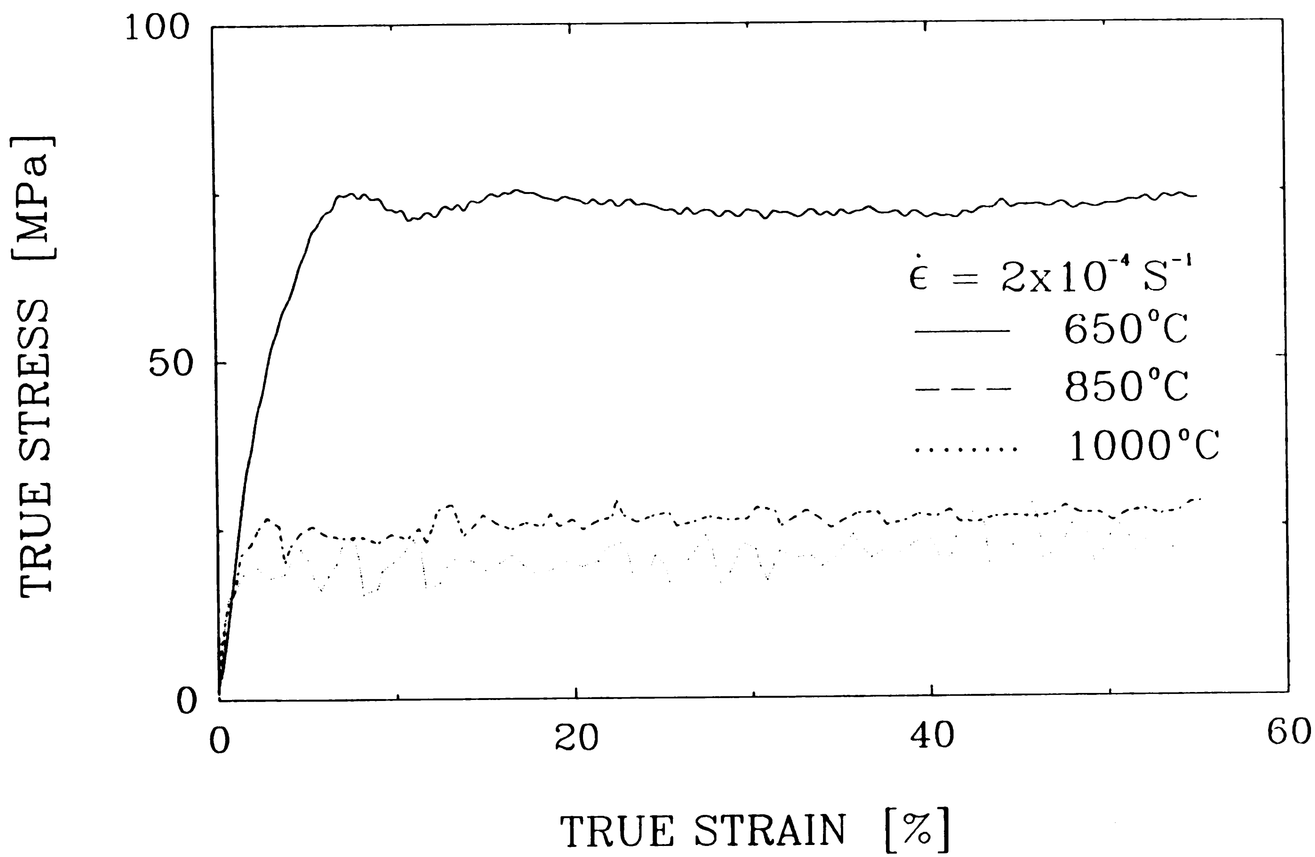

Fig. 17. The flow curves of pure Ni (D_o = 136 μm) which were compressed with strain rate 2 x $10^{-4}S^{-1}$ at various temperatures.

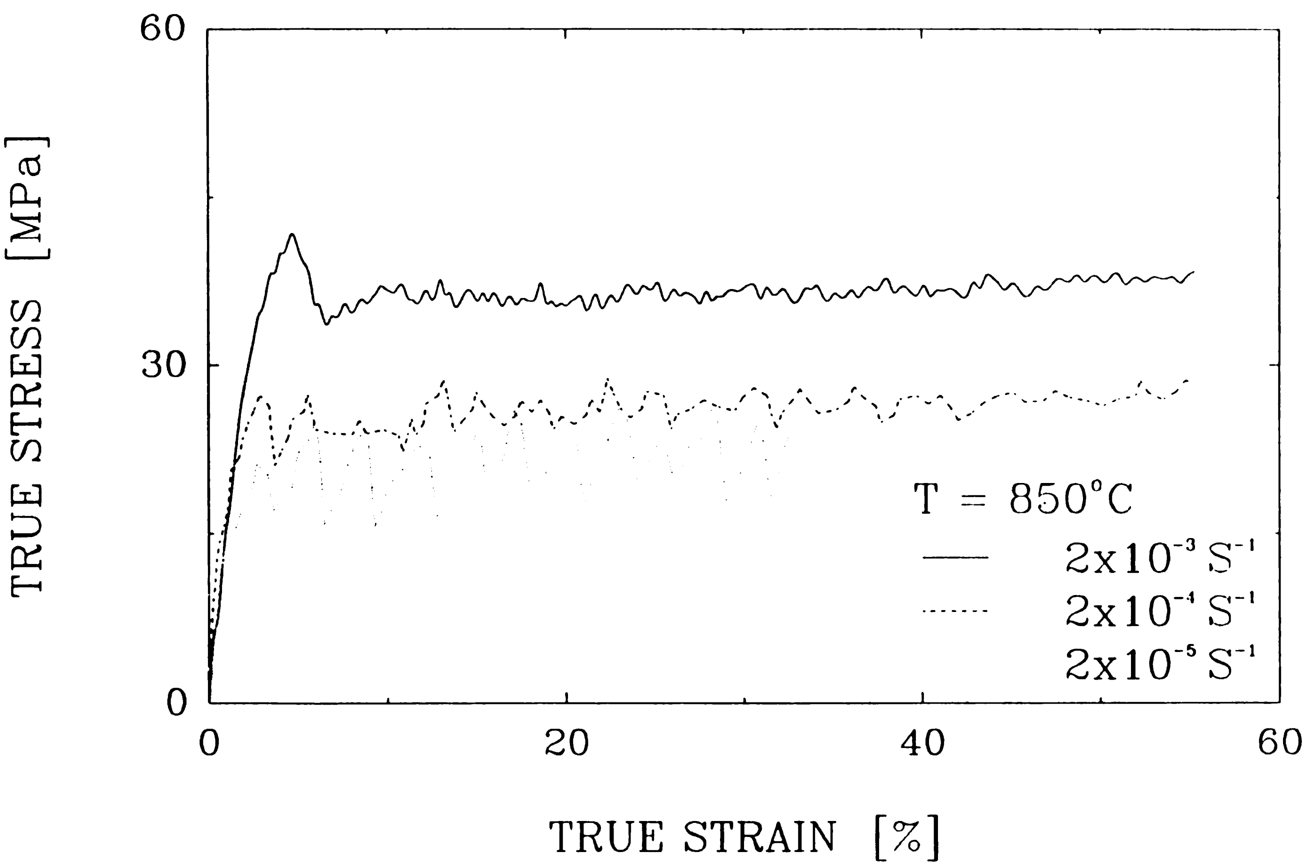

Fig. 18. The flow curves of pure Ni (D_o = 136 μm) which were compressed at 850°C with various strain rates.

Table 3. The σ_R & σ_S under various test condition for pure Ni with D_o = 136 μm.

σ_R (σ_S) \ ε / T°C	$2x10^{-3}s^{-1}$	$2x10^{-4}s^{-1}$	$2x10^{-5}s^{-1}$
650	---	75 (85)	---
850	44 (36)	28 (25)	22 (23)
1000	---	20 (20)	---

Note: The unit for σ_R & σ_S is MPa.

Table 4. The D_S under various test condition for Ni_3Al with D_o = 170 μm.

D_S \ ε / T°C	$2x10^{-3}s^{-1}$	$2x10^{-4}s^{-1}$	$2x10^{-5}s^{-1}$
650	1.7	3	3.5
750	2	2.5	---
850	3	4	6
1000	8	14	30

Note: The unit for D_S is μm.

structure (Fig. 19 - 23) with very tiny nuclei occurs along the original grain boundary while it is subjected to compress at 650°C and 750°C. Until 850°C, the small grains (Fig. 24 - 26)almost grew up within the old grains and replaced them. This phenomenon is remarkable when the strain rate lowered to 2 x $10^{-5}S^{-1}$(Fig. 26). At 1000°C, we can observed that grain growth (Fig. 27 - 29) occurs very strikingly and becomes larger (Fig. 29). Considered the flow curve and compared with the initial grain size (D_o = 170 μm) in Table 4, all of the D_S are much smaller than the D_o , give rise to a single peak flow curve.

As narrated before, the smaller of D_o , the higher of chance of the transition from single peak to multipeak. We prepared a much smaller D_o which was prestrained to 60 % at room temperature and annealed at 800°C for 1 hour to inspect whether the transition would take place or not.

A series of metallographs (Fig. 30 - 35) were taken, we can discover that the D_S is smaller than D_o . The largest one, D_S = 4.4 μm (Table 5), is interesting. Applying the transition criterion, D_o / $2D_S$ = 1, we found the appearance of the single peak behavior. Therefore, all of the curves show the samples undergo the continuous RX process.

As for the pure Ni with D_o = 136 μm , carefully compared with each D_S (Table 6), it is out of question that occur the oscillation RX process (Fig. 36 - 40).

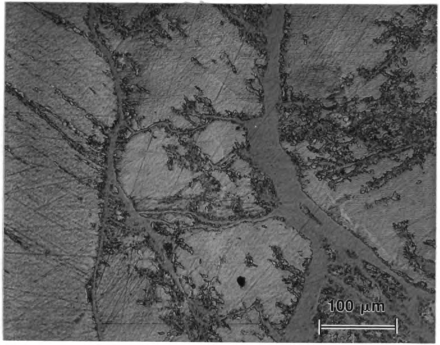

Fig. 19. The metallograph of Ni_3Al (D_0 = 170 µm) after compression test at 650°C with 2 x $10^{-3}S^{-1}$ shows the necklace structure along the existing grain boundary.

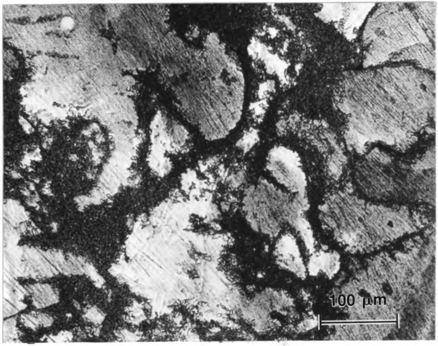

Fig. 20. The metallograph of Ni_3Al (D_o = 170 µm), compressed at 650°C with $2 \times 10^{-4} S^{-1}$, shows the necklace structure along the existing grain boundary.

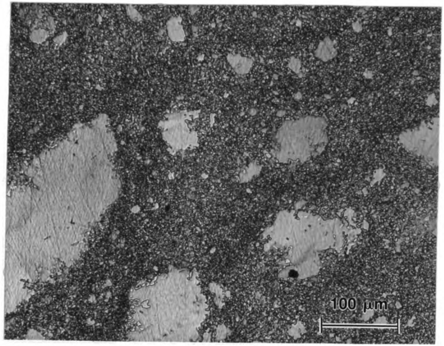

Fig. 21. The metallograph of Ni_3Al (D_o = 170 µm), compressed at 650°C with 2 x $10^{-5}S^{-1}$, shows the necklace along the existing grain boundary.

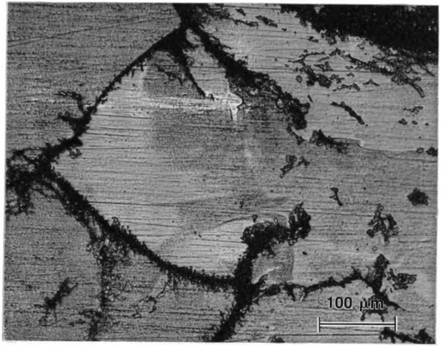

Fig. 22. The metallograph of Ni_3Al (D_o = 170 µm), compressed at 750°C with $2 \times 10^{-3} S^{-1}$, shows the necklace along the existing grain boundary.

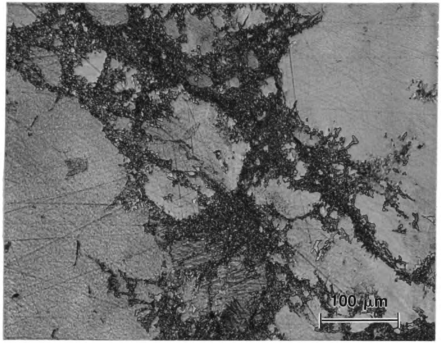

Fig. 23. The metallograph of Ni_3Al (D_o = 170 µm), compressed at 750°C with 2 x $10^{-4}S^{-1}$, shows the necklace along the existing grain boundary.

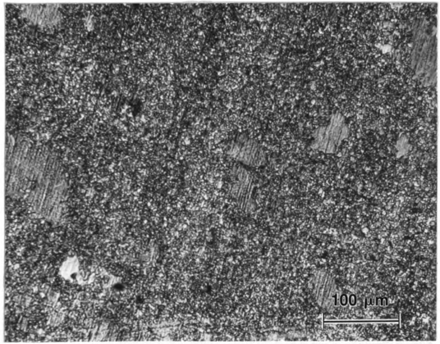

Fig. 24. The metallograph of Ni_3Al (D_o = 170 µm), compressed at 850°C with 2 x $10^{-3}S^{-1}$, shows the grain growth within the necklace.

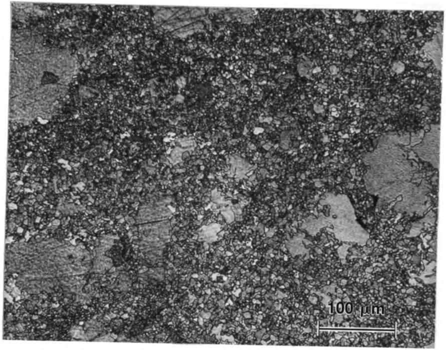

Fig. 25. The metallograph of Ni_3Al (D_o = 170 µm), compressed at 850°C with $2 \times 10^{-4} S^{-1}$.

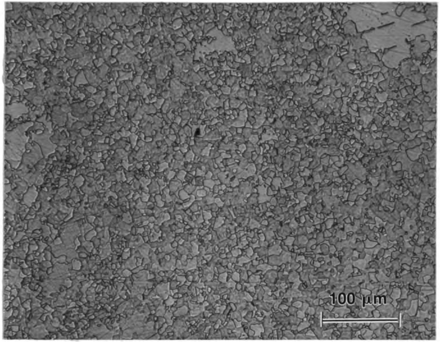

Fig. 26. The metallograph of Ni_3Al (D_o = 170 µm), compressed at 850°C with $2 \times 10^{-5} S^{-1}$.

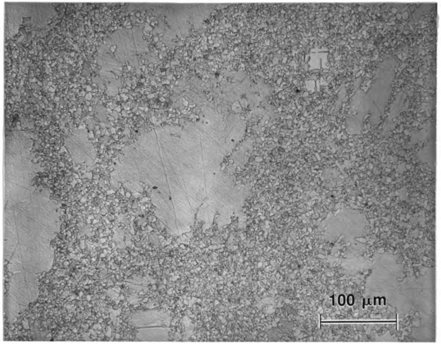

Fig. 27. The metallograph of Ni_3Al (D_o = 170 µm), compressed at 1000°C with $2 \times 10^{-3} S^{-1}$.

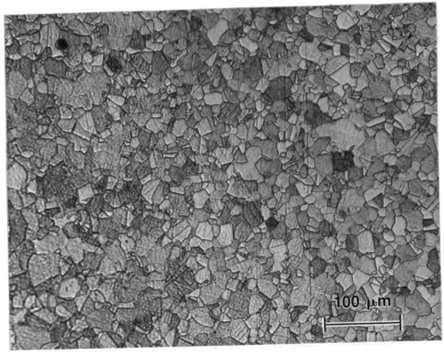

Fig. 28. The metallograph of Ni_3Al (D_o = 170 μm), compressed at 1000°C with 2 x $10^{-4}S^{-1}$.

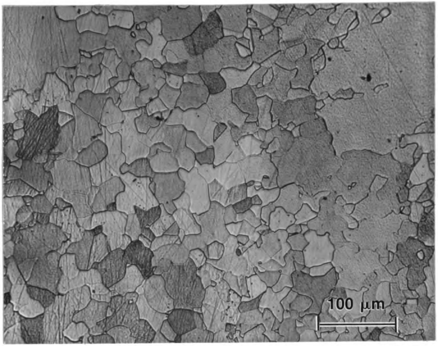

Fig. 29. The metallograph of Ni_3Al (D_o = 170 µm), compressed at 1000°C with $2 \times 10^{-3} s^{-1}$.

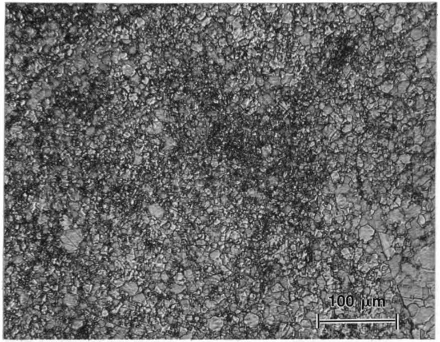

Fig. 30. The metallograph of Ni_3Al (D_o = 9 µm), compressed at 600°C with 2 x $10^{-4}S^{-1}$.

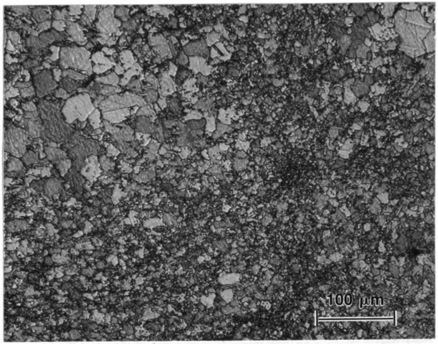

Fig. 31. The metallograph of Ni_3Al (D_o = 9 µm), compressed at 750°C with 2 x $10^{-4}S^{-1}$.

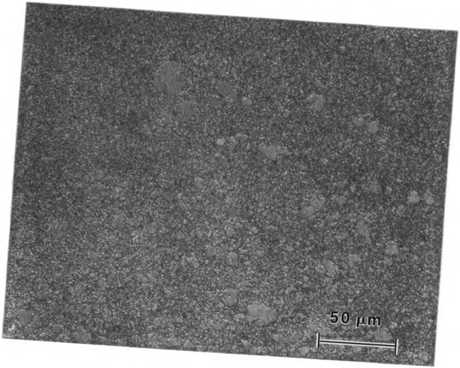

Fig. 32. The metallograph of Ni_3Al (D_o = 9 µm), compressed at 800°C with 2 x $10^{-3}S^{-1}$.

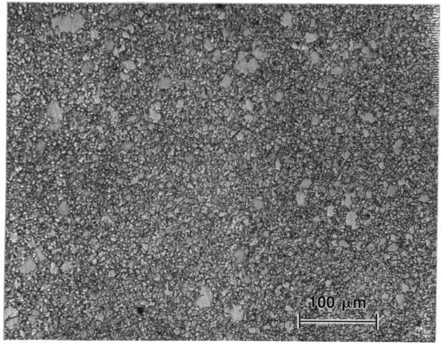

Fig. 33. The metallograph of Ni_3Al (D_o = 9 µm), compressed at 800°C with 2 x $10^{-4}S^{-1}$.

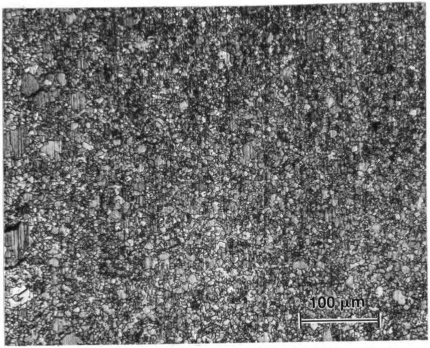

Fig. 34. The metallograph of Ni_3Al (D_o = 9 µm), compressed at 800°C with 7 x $10^{-5}S^{-1}$.

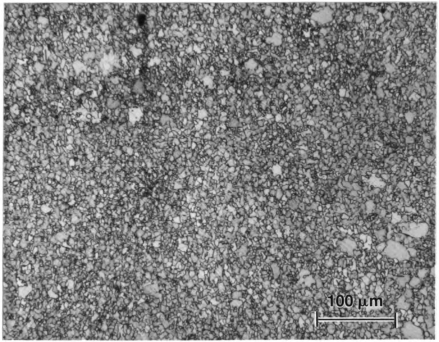

Fig. 35. The metallograph of Ni_3Al (D_o = 9 μm), compressed at 850°C with 2 x $10^{-4}S^{-1}$.

Table 5. The D_S under various test codition for Ni_3Al with D_o = 9 μm.

D_S \ ε / T°C	$2x10^{-3}s^{-1}$	$2x10^{-4}s^{-1}$	$7x10^{-5}s^{-1}$
600	---	1.8	---
750	---	2.3	---
800	2.5	3.3	3.8
850	---	4.4	---

Note: The unit for D_S is μm.

Table 6. The D_S under various test condition for pure Ni with

D_o = 136 μm.

D_S \ ε / T°C	$2x10^{-3}s^{-1}$	$2x10^{-4}s^{-1}$	$2x10^{-5}s^{-1}$
650	---	144	---
850	330	816	911
1000	---	849	---

Note: The unit for D_S is μm.

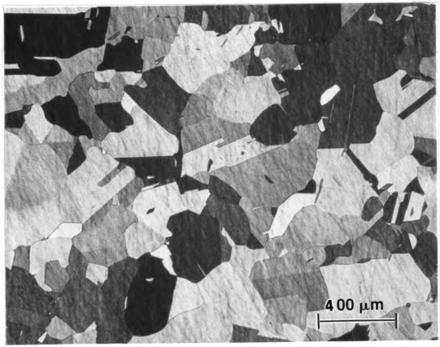

Fig. 36. The metallograph of pure Ni, compressed at 650°C with $2 \times 10^{-4} s^{-1}$.

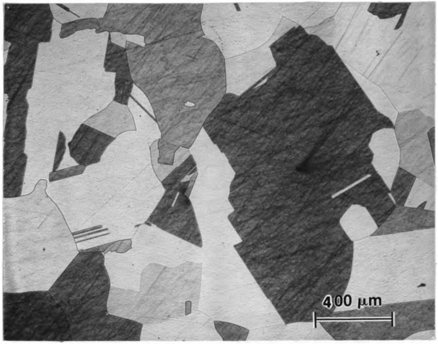

Fig. 37. The metallograph of pure Ni, compressed at 850°C with $2 \times 10^{-3} s^{-1}$.

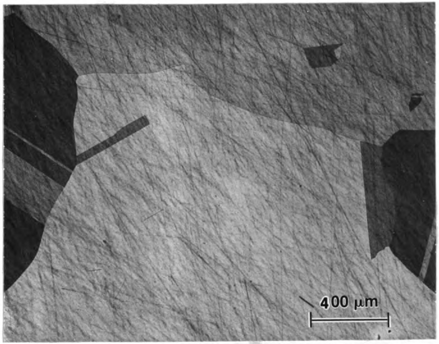

Fig. 38. The metallograph of pure Ni, compressed at 850°C with 2 X $10^{-4}S^{-1}$.

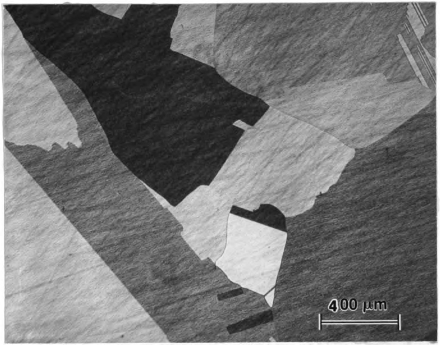

Fig. 39. The metallograph of pure Ni, compressed at 850°C with 2 x $10^{-5}s^{-1}$.

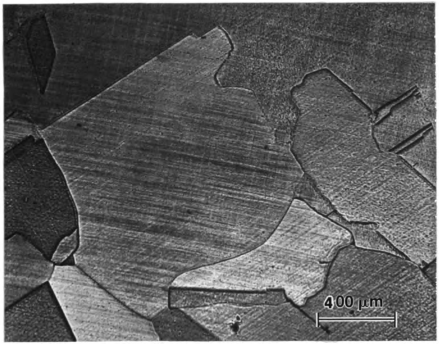

Fig. 40. The metallograph of pure Ni, compressed at 1000°C with 2 x $10^{-4}S^{-1}$.

5. DISCUSSION

5.1 Evidence of the DRX

Due to the $Z = \dot{\varepsilon} \exp (Q / RT)$, we have found that the Z value increases as the increasing $\dot{\varepsilon}$ and reducing temperature, which causes a grain refinement process associated with the single peak flow curve. By contrast, the Z value decreases as decreasing $\dot{\varepsilon}$ and increasing temperature results in a grain coarsening process correspondence to the occurrence of the multipeak flow curve.

In our experiment, only the single peak flow curve appears for Ni_3Al because D_S is much smaller than D_o = 170 μm. Even we prepared a tiny D_o (= 9 μm), the grain refinement showed up because work hardening rate balanced the nucleation rate throughout the deformation process gives rise to the kinetic of growth controlled. Therefore, the dimension of the D_o is independent of the characteristic of the DRX flow curve.

The dependence of the $\dot{\varepsilon}$ & T on σ_R has been plotted for Ni_3Al (Fig. 41 - 44) and Ni (Fig. 45, 46), by an Arhennius - type,

$$\dot{\varepsilon} = A \sigma_R^n \exp (-Q / RT)$$

where, A, n are constants, showing that the RX stress as a function of $\dot{\varepsilon}$ & T. Higher ε and lower T give rise to a higher RX stress.

The peak in flow curve represents the rate of work hardening is just balanced by the rate of softening due to RX [4]. Therefore, the $\dot{\varepsilon}$ and T dependence of the σ_R is determined by the RX process. The activation energy (Q) for RX process can be determined from Fig. 41-43 for Ni_3Al, and 57.79 kcal / mole for pure Ni, determined from Fig.

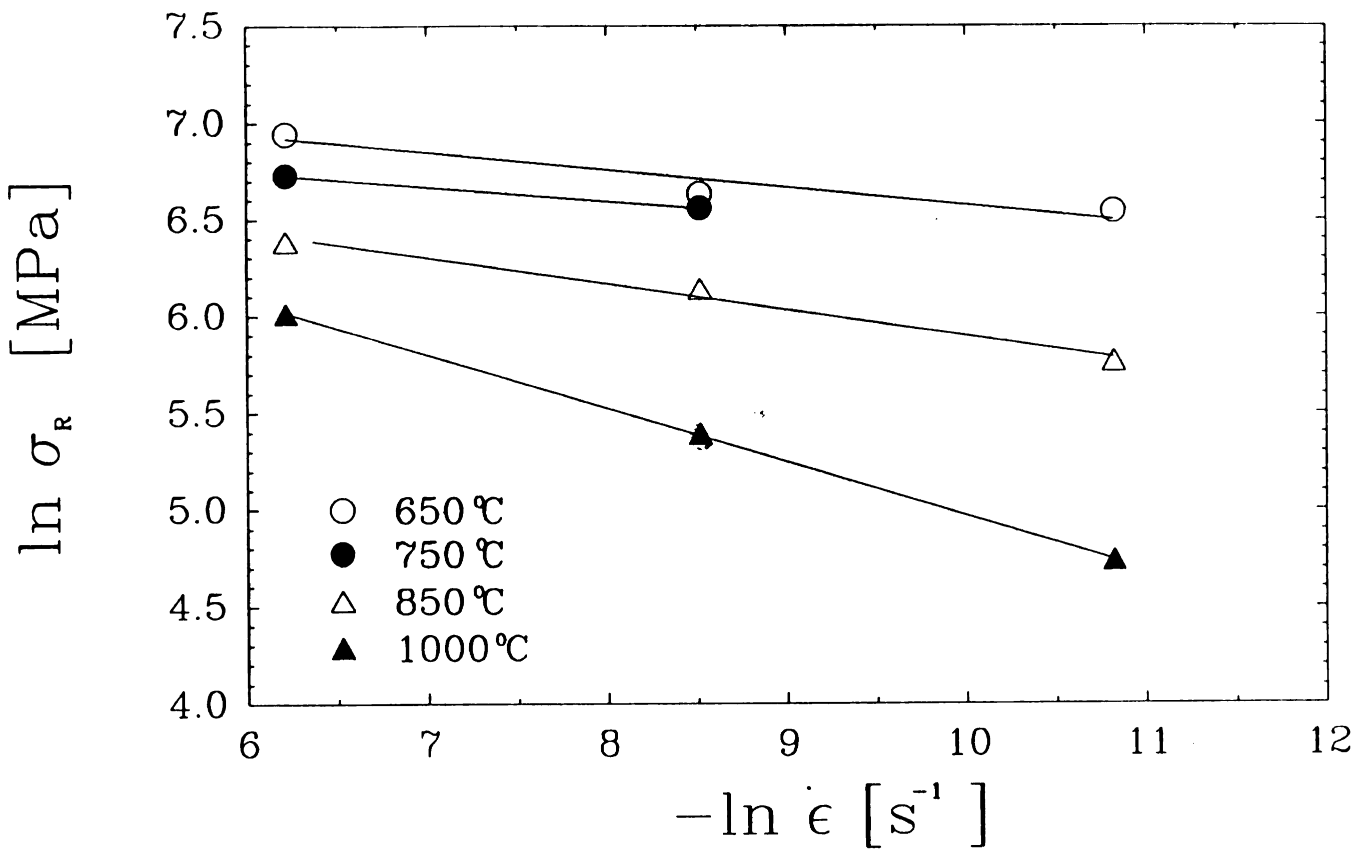

Fig. 41. The relationship of strain rate and σ_R for Ni_3Al with D_o = 170 μm.

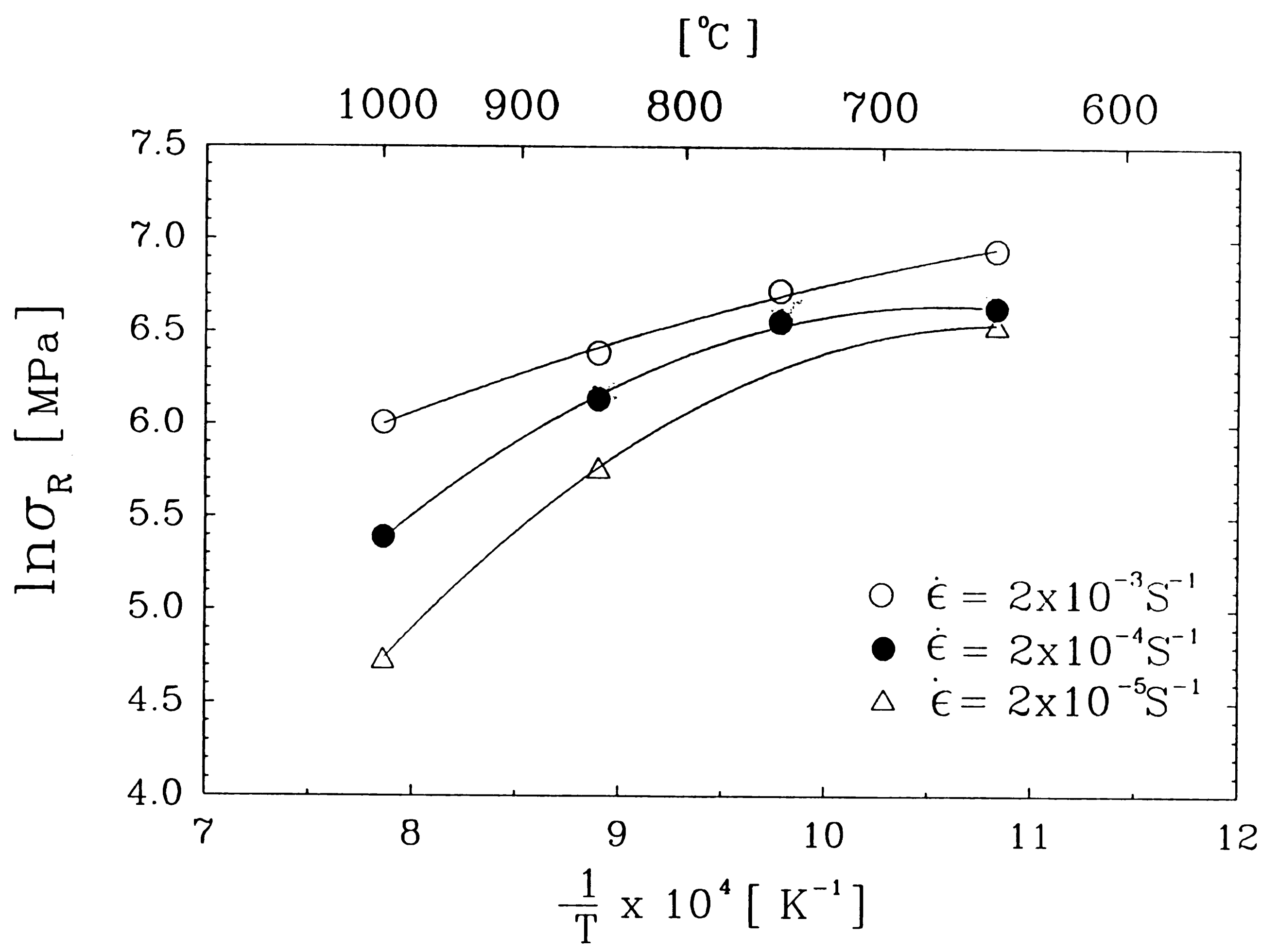

Fig. 42. The relationship of the temperature and σ_R for Ni_3Al with D_o = 170 μm.

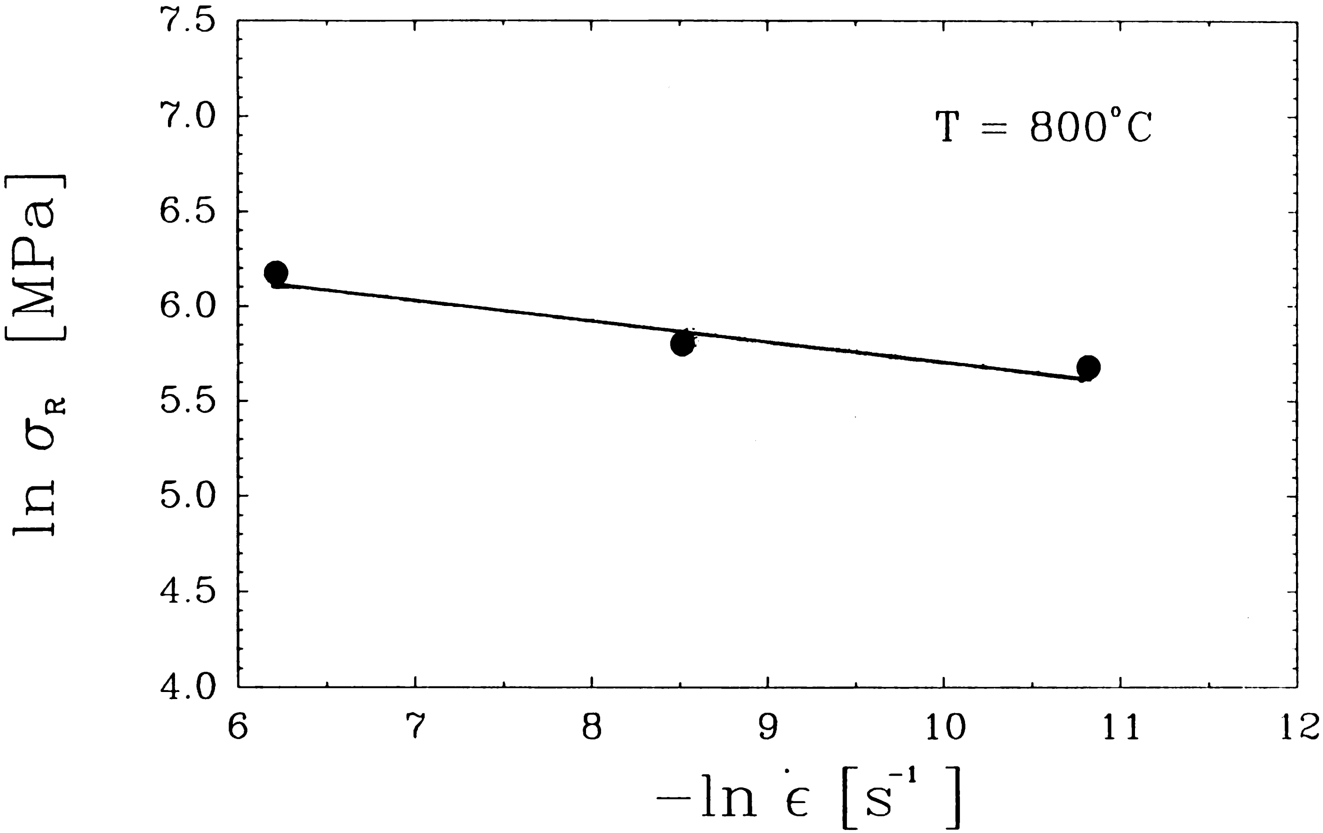

Fig. 43. The relationship of the strain rate and σ_R for Ni_3Al with D_o = 9 μm.

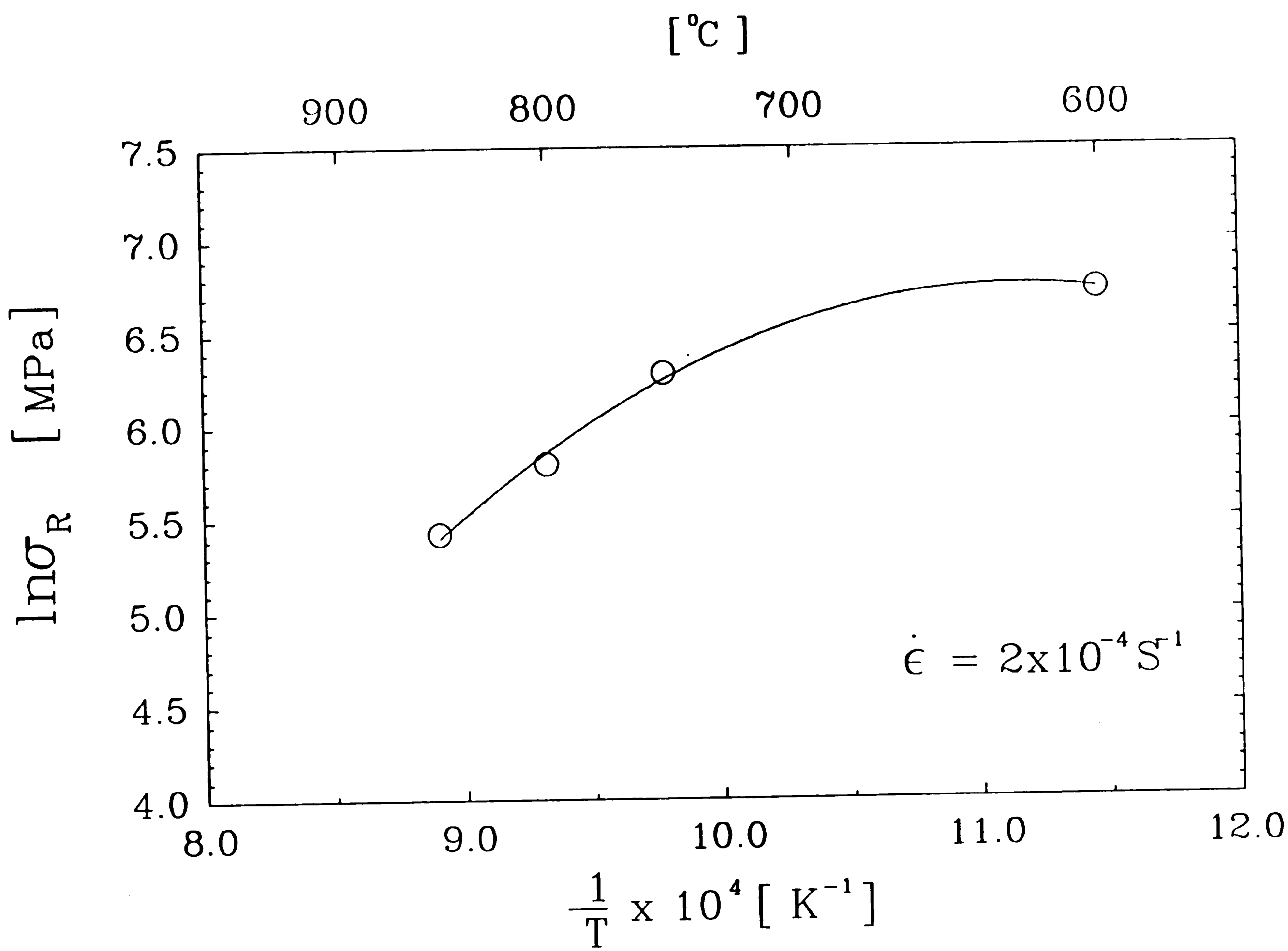

Fig. 44. The relationship of the temperature and σ_R for Ni_3Al with D_o = 9 μm.

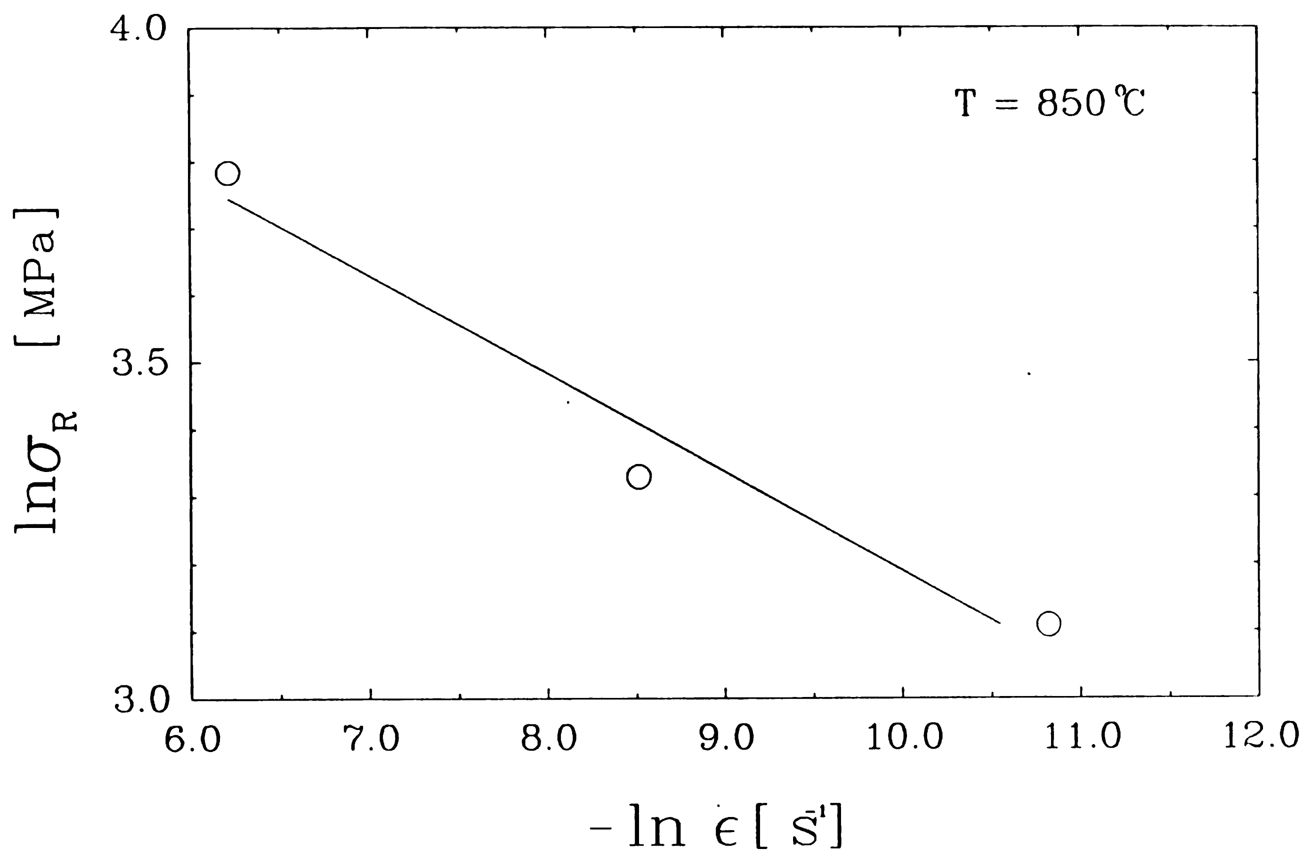

Fig. 45. The relationship of the strain rate and σ_R for pure Ni.

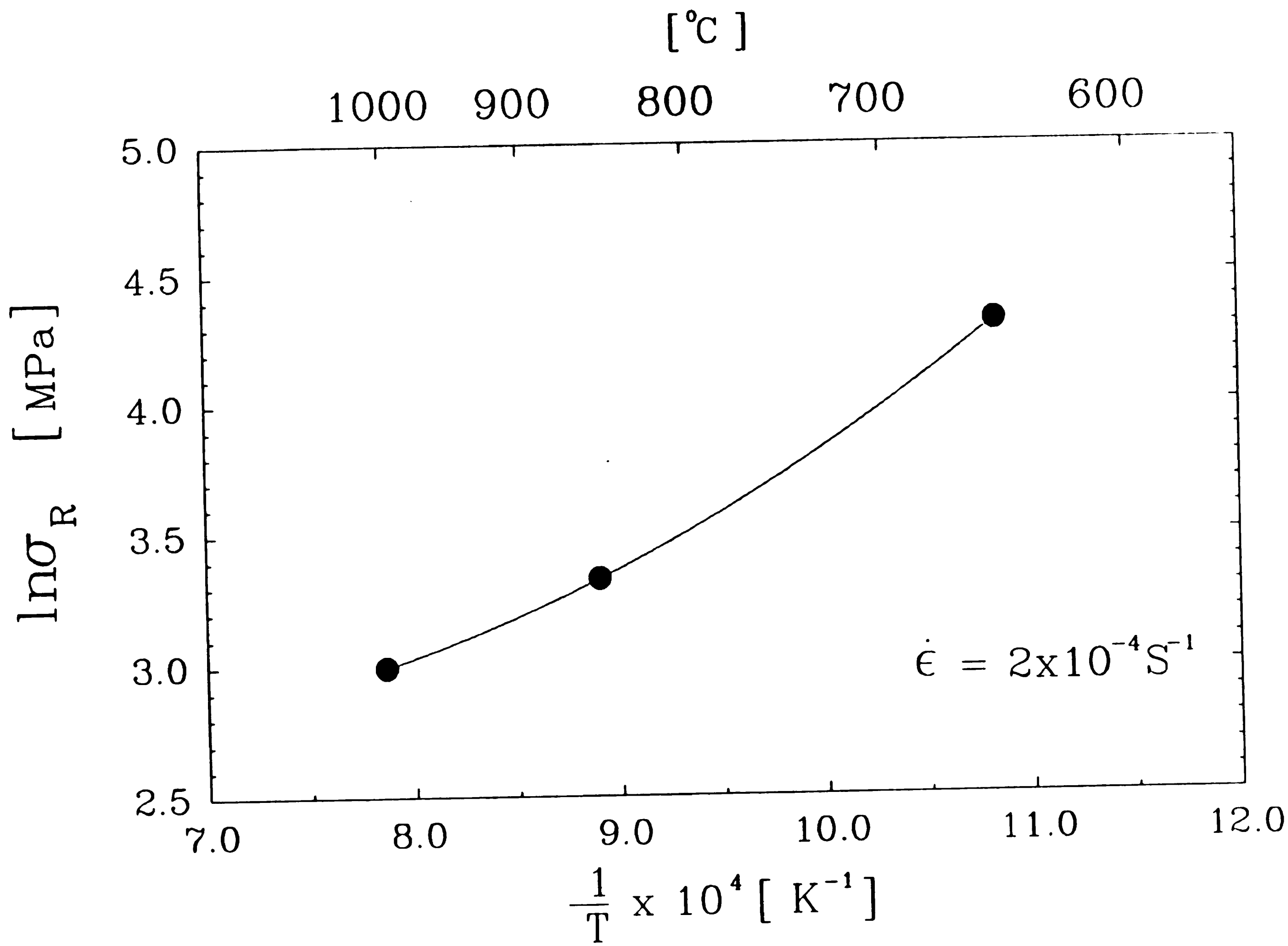

Fig. 46. The relationship of the temperature and σ_R for pure Ni.

45,46. For Ni_3Al, we found the activation energy is different under different test condition. Also, we found that under the same test condition, larger D_o will need larger σ_R to initiate the RX process. The Q = 57.79 kcal / mole for the Ni is very closed to the Luton's result [3], i.e. Q = 56 kcal / mole under hot torsion test.

5.2 The Grain Size of the DRX

The shape of the DRX flow curve is dominated by the transition criterion, $D_o / 2D_S = 1$. Normally, the grain refinement process results from the production of necklace which nucleation takes place at the original boundary. Continuous straining the dynamic recrystallized grains gives rise to the occurrence of another necklace and reduces the growth process of the first necklace structure. Therefore, for Ni_3Al, it is always shows single peak flow curve, under our test condition, due to the grain refinement process.

The grain coarsening process for Ni is owing to the necklace can not be produced along the existing boundary by strain hardening. In this case, the growth of each new dynamic grain is terminated by boundary impingement, and form the metastable with grain Smaller than final grain [3]. Therefore, it makes Ni show the periodic DRX feature.

Consider the σ_S correspondence to D_S , there is an empirical relationship [3,18],

$\sigma_S = \sigma_o + A\, D_S^{-n}$ where, σ_o , A, n are constants. From Fig. 46,47, n = .709 for Ni_3Al and n = .7 for pure Ni, which proves that final grain size only depends on the steady - state flow stress, and does not depend on the material and initial grain size.

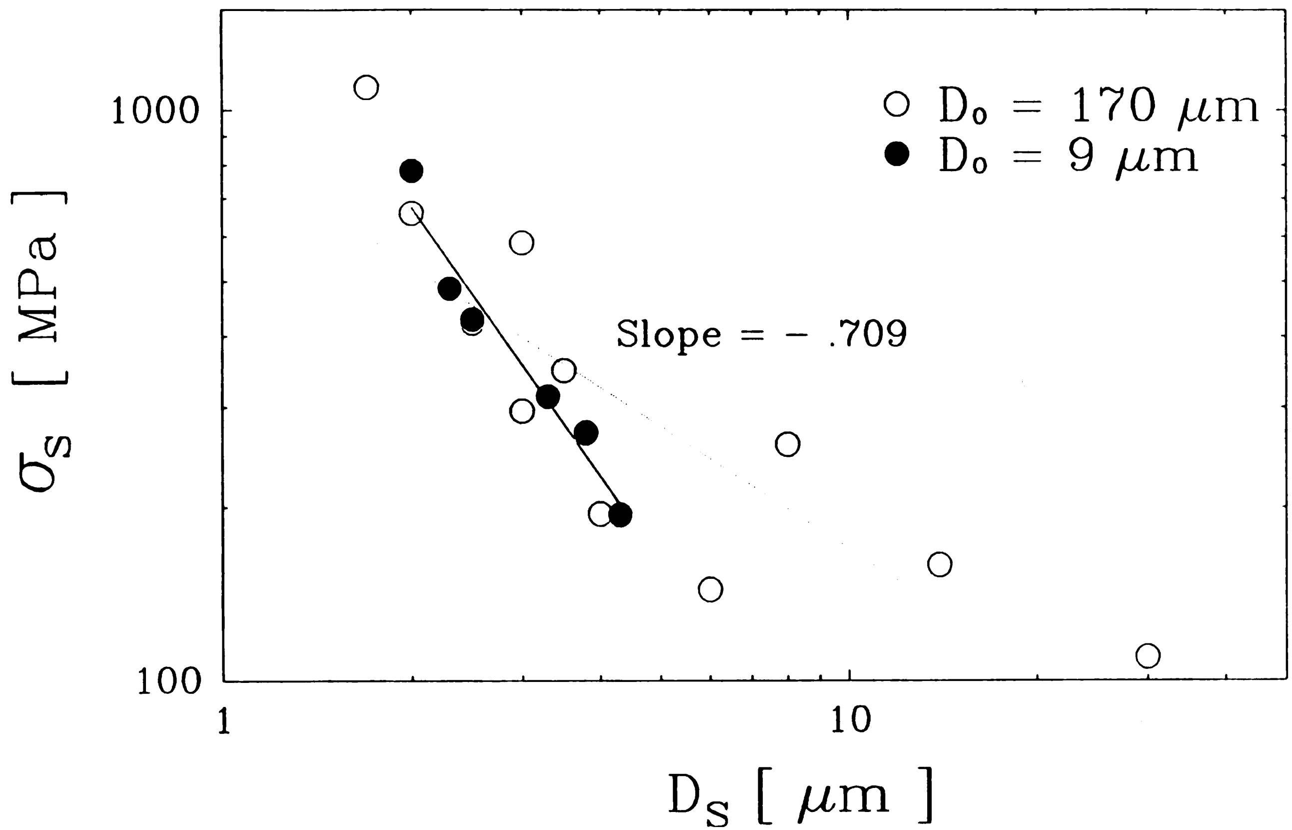

Fig. 47. The relationship of σ_S and final grain size for Ni_3Al.

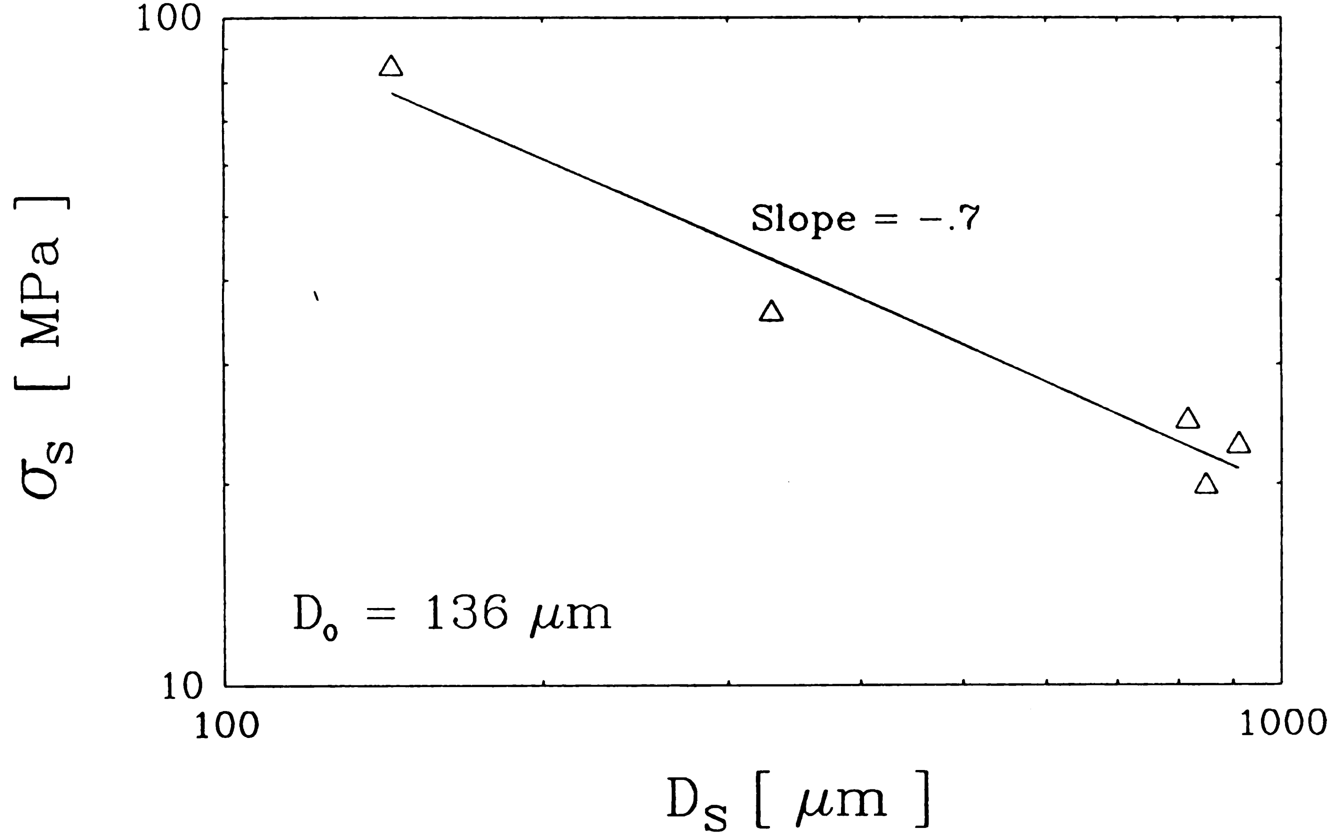

Fig. 48. the relationship of σ_S and final grain size for pure Ni.

6. CONCLUSIONS

The dynamic recrystallization (DRX) behavior of Ni_3Al and pure Ni has been studied during high temperature compression test at different temperatures and strain rates. The results are summarized in the followeing.

1. The DRX behavior is initiated when a certain strss, the recrystallization stress (σ_R) is attained. The σ_R can be changed by changing the Zener - Hollomon parameter $Z = \varepsilon \exp (Q / RT)$. The stress increases with increasing Z i.e. higher strain rate and lower temperature .
2. Under the given conditions, the flow curve of Ni_3Al exhibited always a single maximum. Correspondingly, the microstructure always underwent grain refinement. In contrast, Ni always revealed an oscillating flow curve and correspondingly, always grain coarsening. The resilts are in line with the prediction that a change of flow behavior is only observed
$D_o / 2D_S = 1$.
3. The σ_R was found to decrease with decreasing grain size.
4. A thermal activation analysis yielded the values n = 6.8 and Q = 57.79 kcal / mole for Ni. For Ni_3Al, it was found that n and Q depended on temperature so that a tradition activation analysis is not feasible.
5. In Ni the steady state grain size depended only on the steady state flow stress. The relation is a power law with exponent -0.7. For Ni_3Al it was found that this expinent is not constant but increases strongly for small grain size (< 10 μm).

7. REFERENCES

[1] I. Baker, D. V. Viens and E. M. Schulson : Scripta Metall., vol. 18, 1984, pp. 237 - 240

[2] E. M. Schulson : Met. Trans., vol. 9A, 1978, pp. 527 - 538

[3] T. Sakai and J. J. Jonas : Acta Met., vol. 32, 1984, pp. 189 - 209

[4] M. J. Luton and C. M. Sellars : Acta Met., vol. 17, 1969, pp. 1033 - 1043

[5] H. J. McQueen and S. Bergerson : Met. Sci., vol. 6, 1972, pp. 25 - 29

[6] G. Glover and C. M. Sellars : Met. Trans., vol. 4, 1973, pp. 765 - 775

[7] H. P. Stüve and B. Ortner : Met. Sci., vol. 8, 1974, pp. 161 - 167

[8] J. P. Sah, G. J. Richardson and C. M. Sellars : Met. Sci., vol. 8, 1974, pp. 325 - 331

[9] Rolf Sandström and Rune Lagneborg : Acta Met., vol. 23, 1975, pp. 387 - 398

[10] G. Gottstein, D. Zabardjadi and H. Mecking : Met. Sci., 1979, pp. 223 - 227

[11] G. Gottstein and U. F. Kocks : Acta Met., vol. 31, 1983, pp. 175 - 188

[12] C. M. Sellars and J. A. Whiteman : Met. Sci., 1979, pp. 187 - 194

[13] J. C. Blade : Met. Sci., 1979, pp. 206 - 210

[14] E. L. Brown and A. J. Deardo : Met. Trans., vol. 12A, 1981, pp. 39 - 47

[15] W. Roberts, H. Boden and B. Ahlblom : Met. Sci., 1979, pp. 195 - 2.5

[16] K. J. Gardner and R. Grimes : Met. Sci., 1979, pp. 216 - 222

[17] M. G. Akbén, I. Weiss and J. J. Jonas : Acta Met., vol. 29, 1981, pp. 111 - 121

[18] T. Sakai, M. G. Akben and J. J. Jonas : Acta Met., vol. 31, 1983, pp. 631 - 641

[19] H. J. McQueen and J. J. Jonas in " Recovery and Recrystallization During High Temperature Deformation " in Treatise on Materials Science and Technology, vol. 6, 1975, pp. 393 - 493